DEPARTMENT OF PHYSICS
UNIVERSITY OF JYVÄSKYLÄ
RESEARCH REPORT No. 1/2013

IMPROVED LATTICE ACTIONS FOR BEYOND THE STANDARD MODEL PHYSICS

BY
TUOMAS KARAVIRTA

Academic Dissertation
for the Degree of
Doctor of Philosophy

To be presented, by permission of the
Faculty of Mathematics and Science
of the University of Jyväskylä,
for public examination in Auditorium FYS-1 of the
University of Jyväskylä on January 18, 2013
at 12 o'clock noon

Jyväskylä, Finland
January 2013

ISBN 978-951-39-5040-8 (nid.)
ISBN 978-951-39-9172-2 (PDF)

Preface

The research for this thesis was done at the Department of physics at the University of Jyväskylä during 2008-2013. I would like to thank my supervisors Doc. Kimmo Tuominen and Prof. Kari Rummukainen for introducing me to the interesting world of lattice field theory and sharing their knowledge with me. I am grateful to Prof. Keijo Kajantie and Dr. Ari Hietanen for their valuable comments regarding the manuscript, and to Dr. Antonio Rago for agreeing to be my opponent. Most of the research that led to this thesis was done in collaboration with Dr. Jarno Rantaharju and Dr. Anne-Mari Mykkänen to whom I want to express my gratitude.

The department of physics at the university of Jyväskylä has been an excellent place for studying physics and doing research. I am thankful to all the faculty members that have contributed to my education and to the office personnel who have helped me during my years in the department of physics. I would also like to thank my fellow Ph.D. students for countless discussions about physics and other less scientific subjects. Last but not least I would like to thank my family and especially my wife Tiina for their love and support.

This thesis was supported by the Ellen and Artturi Nyyssönen foundation, the Magnus Ehrnrooth foundation, the faculty of Mathematics and Science at the University of Jyväskylä and the Helsinki Institute of Physics.

List of publications

This thesis is based on the following publications:

I **Nonperturbative improvement of SU(2) lattice gauge theory with adjoint or fundamental flavors**
T. Karavirta, A. Mykkanen, J. Rantaharju, K. Rummukainen and K. Tuominen,
JHEP **1106**, 061 (2011) [arXiv:1101.0154 [hep-lat]].

II **Perturbative Improvement of the Schrodinger Functional for Lattice Strong Dynamics**
T. Karavirta, K. Rummukainen and K. Tuominen,
Phys. Rev. D **85**, 054506 (2012) [arXiv:1201.1883 [hep-lat]].

III **Determining the conformal window: SU(2) gauge theory with N_f = 4, 6 and 10 fermion flavours**
T. Karavirta, J. Rantaharju, K. Rummukainen and K. Tuominen,
JHEP **1205**, 003 (2012) [arXiv:1111.4104 [hep-lat]].

The author has done the perturbative calculations in papers I and II, the $N_F = 10$ simulations in paper III and participated in the analysis of the data and writing of all the papers.

Contents

Chapter 1

Introduction: The standard model and beyond

The Standard Model (SM) of particle physics is one of the most accurate theories in physics. It describes three of the four known fundamental interactions; strong and weak nuclear force and electromagnetism (EM). Gravity is the only fundamental interaction not included in SM. After years of experiments, including the recent discovery of a boson with mass 125 GeV, SM is still compatible with the experimental data.

In SM, the interactions arise from local gauge symmetries. In the case of EM, the underlying local symmetry is U(1). For the fermionic fields $\psi(x)$ this symmetry transformation is

$$\psi(x) \to \exp[\mathrm{i}e\omega(x)]\psi(x), \tag{1.1}$$

where $\omega(x)$ is an arbitrary continuously differentiable function and e is the coupling constant of the theory that describes the strength of the coupling between the fermionic field $\psi(x)$ and the gauge field $A_\mu(x)$. The Lagrangian

$$\mathcal{L}_F = \bar{\psi}(x)\left[(\mathrm{i}\partial_\mu + eA_\mu)\gamma^\mu - m\right]\psi(x), \tag{1.2}$$

is now invariant under the U(1) transformation (1.1), if the gauge field $A_\mu(x)$ transforms as

$$A_\mu(x) \to A_\mu(x) + \partial_\mu\omega(x). \tag{1.3}$$

The proper kinetic term for the gauge field $A_\mu(x)$, which describes the kinematics of the gauge boson of EM, should also be added to the Lagrangian. It is

$$\mathcal{L}_G = -\frac{1}{4}F^{\mu\nu}F_{\mu\nu}, \tag{1.4}$$

where the field strength tensor $F_{\mu\nu} = \partial_\mu A_\nu(x) - \partial_\nu A_\mu(x)$. The gauge field $A_\mu(x)$, called photon, is the mediator of the EM interaction. The two terms, (1.2) and (1.4), form the Lagrangian of Quantum Electrodynamics (QED).

The same gauge principle applies to other gauge symmetry groups as well. SM is $\mathrm{SU(3)}\times\mathrm{SU(2)}\times\mathrm{U(1)}$ symmetric gauge theory, where the symmetry group $\mathrm{SU(3)}$ corresponds to the strong interaction, the theoretical formulation of which is known as quantum chromodynamics (QCD). The gauge group $\mathrm{SU_T(2)}\times\mathrm{U_Y(1)}$, where $\mathrm{SU_T(2)}$ is the weak isospin and $\mathrm{U_Y(1)}$ is the weak hypercharge symmetry, corresponds to the electro-weak interaction, which is spontaneously broken down to $\mathrm{U_{EM}(1)}$ of EM. The elementary matter particles in SM are quarks and leptons, all of which have an anti-particle with opposite quantum numbers. In addition there are gauge bosons that mediate these interactions[1]: gluons (strong nuclear), $\mathrm{W^{\pm}}$- and Z-bosons (weak nuclear) and photons (EM).The EM interaction couples to both quarks and leptons and the strong interaction only to quarks. To explain which particles interact through weak interaction, a property called chirality must be introduced.

Chirality of a particle is defined to be left (right) handed, if the particle transforms in left (right) handed representation of the Poincaré group. The left- and right handed fermionic fields are defined as

$$\psi_L = \frac{1-\gamma_5}{2}\psi, \qquad \psi_R = \frac{1+\gamma_5}{2}\psi, \tag{1.5}$$

where $\psi = \psi_L + \psi_R$ and the chirality transformation is

$$\psi_L \to e^{-\frac{\mathrm{i}}{2}\theta_L}\psi_L, \qquad \psi_R \to e^{-\frac{\mathrm{i}}{2}\theta_R}\psi_R. \tag{1.6}$$

Chirality is important because the weak interaction couples only to the left handed particles. This means that left handed particles are organized into $\mathrm{SU(2)}$ doublets and right handed particles to $\mathrm{SU(2)}$ singlets under the weak interaction. These can be expressed as

$$Q_L = \begin{pmatrix} u_L \\ d_L \end{pmatrix}, \quad E_L = \begin{pmatrix} e_L \\ (\nu_e)_L \end{pmatrix}, \quad u_R, \quad d_R, \quad e_R. \tag{1.7}$$

The other generations of quarks and leptons are organized similarly. Because the left and right handed fields transform differently under the $\mathrm{SU(2)}$ gauge transformation, the mass terms that are of the form $m(\bar{\psi}_L\psi_R + \bar{\psi}_R\psi_L)$ are not invariant in this gauge transformation.The mass terms for the gauge bosons are also not invariant under the $\mathrm{SU(2)}$ gauge transformation. This means that mass terms for weak gauge bosons and matter particles can not appear in this theory. However, according to experiments, the three gauge bosons ($\mathrm{W^{\pm}}$ and Z) of the weak interaction are massive, as are quarks, electrons, muons and taus. In SM the masses of the gauge bosons and matter particles are introduced through electroweak symmetry breaking and the associated Higgs mechanism.

[1]The number of gauge bosons is the same as the number of generators in the corresponding gauge group, thus there are eight gluons, three weak bosons and the photon.

1.1 Higgs mechanism

In SM the weak and EM forces are unified to one electroweak (EW) interaction. This EW interaction has $\mathrm{SU_T}(2)\times\mathrm{U_Y}(1)$ gauge symmetry. We introduce a new scalar doublet ϕ to SM with Lagrangian

$$\mathcal{L}_H = |D_\mu\phi|^2 - \mu^2\phi^\dagger\phi - \lambda(\phi^\dagger\phi)^2, \tag{1.8}$$

where $\lambda > 0$, and $\mu^2 < 0$, giving the wrong sign for the mass term. This couples to the EW sector through the covariant derivative

$$D_\mu = \partial_\mu - \mathrm{i}gA^a_\mu\tau^a - \mathrm{i}\frac{g'}{2}B_\mu, \tag{1.9}$$

where τ^a are the generators of $\mathrm{SU_T}(2)$. The Lagrangian (1.9) is invariant under $\mathrm{SU_T}(2)\times\mathrm{U_Y}(1)$ transformation

$$\phi \to \exp(\mathrm{i}\vec{\alpha}\cdot\vec{\tau})\exp(\mathrm{i}\beta/2)\phi, \tag{1.10}$$

where $\vec{\alpha}\in\mathbb{R}^3, \beta\in\mathbb{R}$ are arbitrary. The derivative of the potential

$$V = \mu^2\phi^\dagger\phi + \lambda(\phi^\dagger\phi)^2, \tag{1.11}$$

has two zeros. The point $\phi = 0$ is a local maximum and $|\phi|^2 = \frac{-\mu^2}{2\lambda} = v^2$ is a minimum of the potential V. Thus, the vacuum expectation value of the field ϕ is nonzero. The physical vacuum of the system is the minimum of the potential and so we must expand the Lagrangian around it. The field ϕ can be written as

$$\phi(x) = \frac{1}{\sqrt{2}}\begin{pmatrix} \pi_1(x) + \mathrm{i}\pi_2(x) \\ \sqrt{2}v + \sigma(x) + \mathrm{i}\pi_3(x) \end{pmatrix}, \tag{1.12}$$

where fields $\pi_i(x)$ and $\sigma(x)$ are real.

If we now write the potential V from (1.11) using (1.12) and drop terms that do not depend on x we get

$$V = -\mu^2\sigma^2 + \frac{\lambda}{4}(\pi_i^2)^2 + \sqrt{2}v\lambda\sigma\pi_i^2 + \frac{\lambda}{2}\sigma^2\pi_i^2 + \sqrt{2}v\lambda\sigma^3 + \frac{\lambda}{4}\sigma^4. \tag{1.13}$$

The mass term of the field σ now has the right sign and the other components π_i are massless. From the covariant derivative we get

$$\begin{aligned} |D_\mu\phi|^2 &= \frac{1}{2}\left[(\partial_\mu\pi_i)^2 + (\partial_\mu\sigma)^2\right] + \frac{1}{8}\left[(A_1^2 + A_2^2)g^2\pi_i^2 + \sigma^2)\right] \\ &+ \frac{1}{8}\left[(gA_\mu^3 + g'B_\mu)^2(\pi_1^2 + \pi_2^2) + (gA_\mu^3 - g'B_\mu)^2(\sigma^2 + \pi_3^2)\right] \\ &+ \frac{1}{8}(v^2 + 2v\sigma)\left[(A_1^2 + A_2^2)g^2 + (gA_\mu^3 - g'B_\mu)^2\right] + \ldots, \end{aligned} \tag{1.14}$$

where we have excluded interaction terms involving fields π_i and $\partial_\mu \pi_i$, that are uninteresting at the moment. We define new fields

$$\begin{aligned} W_\mu^\pm &= \tfrac{1}{\sqrt{2}}(A_\mu^1 \mp \mathrm{i} A_\mu^2), \\ Z_\mu^0 &= \tfrac{1}{\sqrt{g^2+g'^2}}(g A_\mu^3 - g' B_\mu), \\ A_\mu &= \tfrac{1}{\sqrt{g^2+g'^2}}(g' A_\mu^3 + g B_\mu), \end{aligned} \tag{1.15}$$

which are the gauge bosons for weak ($W_\mu^\pm$ and Z_μ^0) and EM (A_μ) interactions. Inserting these to (1.14) results in

$$\begin{aligned} |D_\mu \phi|^2 &= \frac{1}{2}\left[(\partial_\mu \pi_i)^2 + (\partial_\mu \sigma)^2\right] + \frac{1}{8}\left[(|W_\mu^+|^2 + |W_\mu^-|^2) g^2 (\pi_i^2 + \sigma^2)\right] \\ &+ \frac{1}{8(g^2+g'^2)}\left[(g^2 - g'^2) Z_\mu^0 + 2 g g' A_\mu\right]^2 (\pi_1^2 + \pi_2^2) \\ &+ \frac{1}{8}\left[(g^2+g'^2)|Z_\mu^0|^2 (\sigma^2 + \pi_3^2)\right] \\ &+ \frac{1}{8}(v^2 + 2v\sigma)\left[(|W_\mu^+|^2 + |W_\mu^-|^2) g^2 + (g^2+g'^2)|Z_\mu^0|^2\right] + \ldots \end{aligned} \tag{1.16}$$

where we find the mass terms for the weak gauge bosons. These masses are

$$M_W^2 = \frac{v^2 g^2}{4}, \qquad M_Z^2 = \frac{v^2 (g^2 + g'^2)}{4}, \tag{1.17}$$

while the photon remains massless. The field σ is called the Higgs field and its excitation is the Higgs boson.

The Lagrangian that we got by expanding (1.9) around its physical vacuum is no longer invariant under the $\mathrm{SU_T(2)}\times\mathrm{U_Y(1)}$ transformation (1.10). However it is invariant under $\mathrm{U_{EM}(1)}$ transformations of the field A_μ *i.e.* we have spontaneously broken the $\mathrm{SU_T(2)}\times\mathrm{U_Y(1)}$ symmetry down to $\mathrm{U_{EM}(1)}$.

The previously shown formalism was first applied to scalar QED by P. Higgs in 1964 [1, 2]. It was first applied to electro-weak symmetry breaking independently in 1967 by S. Weinberg [3], in 1968 by A. Salam [4] and in 1970 by S. L. Glashow *et al.* [5]. Glashow, Weinberg and Salam received the Nobel prize for their work in 1979. The Higgs boson, included in these theories, is the last undiscovered particle in SM. In July 2012 the experimental teams CMS and ATLAS at the Large Hadron Collider (LHC) in CERN announced a discovery of a new Higgs-like particle with a mass between $125 - 127$ GeV [6, 7].

The masses of the fermions are introduced to the SM with Yukawa couplings between left- and right handed fermions and the field ϕ. The terms

$$-\lambda_d\Big(\bar{Q}_L \phi d_R + \bar{d}_R \phi^\dagger Q_L\Big) - \lambda_u\Big(\bar{Q}_L \tilde{\phi} u_R + \bar{u}_R \tilde{\phi}^\dagger Q_L\Big), \tag{1.18}$$

where $\tilde{\phi} = \mathrm{i}\sigma_2 \phi^*$ and $\sigma_2 = \begin{pmatrix} 0 & -\mathrm{i} \\ \mathrm{i} & 0 \end{pmatrix}$ is the second Pauli matrix, are invariant in $\mathrm{SU(2)}\times\mathrm{U(1)}$ transformations and can be added to the Lagrangian. If we

expand the mass terms (1.18) around the physical vacuum *i.e.* inserting (1.12) we get

$$-\frac{\lambda_d v}{\sqrt{2}}\Big(\bar{d}_L d_R + \bar{d}_R d_L\Big) - \frac{\lambda_u v}{\sqrt{2}}\Big(\bar{u}_L u_R + \bar{u}_R u_L\Big) + \ldots, \tag{1.19}$$

which are mass terms for u- and d quark with $m_u = \lambda_u v/\sqrt{2}$ and $m_d = \lambda_d v/\sqrt{2}$. Similar terms can be added for other quark generations and leptons as well. We have now included masses for the matter particles in the SM in a gauge invariant way.

There are two problems with the mathematical formulation of a fundamental scalar field such as the Higgs field. The first is triviality: If the cut off scale, meaning the scale above which the theory is not applicable, is taken to infinity the coupling of the scalar field is identically zero. The second is fine tuning: The mass of a scalar particle is renormalized additively. This leads to the problem that the mass of a fundamental scalar particle has to be fine tuned extremely accurately order by order in perturbation theory to keep the mass of the particle at any finite value.

1.2 Mathematical formalism of $\mathrm{SU}(N_\mathrm{C})$ gauge theory

In the continuum the action of $\mathrm{SU}(N_\mathrm{C})$ gauge theory, where N_C is the number of color degrees of freedom, is

$$\begin{aligned} S &= S_\mathrm{G} + S_\mathrm{F}, & (1.20)\\ S_\mathrm{G} &= \int -\frac{1}{4} F^a_{\mu\nu} F_a^{\mu\nu} d^4x, & (1.21)\\ S_\mathrm{F} &= \int \bar{\psi}(\mathrm{i}D_\mu \gamma^\mu - m)\psi d^4x, & (1.22) \end{aligned}$$

where the fermionic fields ψ can be in any representation R of the gauge group $\mathrm{SU}(N_\mathrm{C})$. The action involves the covariant derivative

$$D_\mu = \partial_\mu - \mathrm{i}g A^a_\mu T^a_R, \tag{1.23}$$

where T^a_R are the generators of $\mathrm{SU}(N_\mathrm{C})$ in representation R. The field strength tensor $F^a_{\mu\nu}$ can be derived from

$$[D_\mu, D_\nu] = -\mathrm{i}g F^a_{\mu\nu} T^a_R, \tag{1.24}$$

and it is

$$F^a_{\mu\nu} = \partial_\mu A^a_\nu - \partial_\nu A^a_\mu + g f^{abc} A^b_\mu A^c_\nu, \tag{1.25}$$

where f^{abc} are the structure constants of the corresponding gauge group $\mathrm{SU}(N_\mathrm{C})$.

For complex representations R the theory has a $\mathrm{SU_L}(N_\mathrm{F}) \times \mathrm{SU_R}(N_\mathrm{F})$ chiral symmetry[2] in the limit of N_F massless fermions. The chiral transformation is

$$\psi_L \to e^{-\frac{\mathrm{i}}{2}\vec{\theta}_L\cdot\vec{\tau}}\psi_L, \qquad \psi_R \to e^{-\frac{\mathrm{i}}{2}\vec{\theta}_R\cdot\vec{\tau}}\psi_R, \tag{1.26}$$

where the matrices τ_a are the generators of the group $\mathrm{SU}(N_\mathrm{F})$ and $\vec{\theta} \in \mathbb{R}^{N_\mathrm{F}}$ is arbitrary. The action (1.22) with $m = 0$ is symmetric under this transformation.

In QCD (and QCD-like theories) the chiral symmetry is spontaneously broken in the vacuum due to the quark-antiquark condensate. If the representation R is complex, the $\mathrm{SU_L}(N_\mathrm{F}) \times \mathrm{SU_R}(N_\mathrm{F})$ chiral symmetry breaks down to $\mathrm{SU}(N_\mathrm{F})$[3]. The pions are the Goldstone bosons corresponding to the spontaneously broken chiral symmetry. The number of pions is $N_\mathrm{F}^2 - 1$ for complex representations[4]. Due to the small masses of the two lightest fermion flavors, the pions also have a small mass. If the fermions were massless, so would be the pions.

1.3 Technicolor

There is a mechanism that generates masses for the gauge bosons in QCD. Similarly to the mechanism of superconductivity, where electrons condense and form Cooper pairs, the quarks and anti-quarks form quark-antiquark $\langle\bar{q}q\rangle$ condensate. This condensate breaks the $\mathrm{SU_L}(2)\times\mathrm{SU_R}(2)$ chiral symmetry in the QCD vacuum down to residual $\mathrm{SU}(2)$ symmetry and as a consequence three massless Goldstone bosons ($\pi^\pm$ and π^0) appear.

If we treat the mesons[5] $\sigma = \bar{q}q$ and $\pi_a = \bar{q}\mathrm{i}\tau_a\gamma_5 q$ as the fundamental degrees of freedom we can write an effective Lagrangian for QCD in the form

$$\mathcal{L} = |D_\mu\phi|^2 - \mu^2\phi^\dagger\phi - \lambda(\phi^\dagger\phi)^2, \tag{1.27}$$

where $\mu^2 < 0$ and

$$\phi(x) = \frac{1}{\sqrt{2}}\begin{pmatrix} \pi_1(x) + \mathrm{i}\pi_2(x) \\ \sqrt{2}v + \sigma(x) + \mathrm{i}\pi_3(x) \end{pmatrix}. \tag{1.28}$$

The situation is completely analogous to the Higgs mechanism in section 1.1. Now the σ field has a vacuum expectation value $v = f_\pi \approx 95$ MeV and inserting this to (1.17), with the assumption $g = 0.65$, we get $M_W \approx 30$ MeV. This is roughly three orders of magnitude smaller than the observed mass $M_W =$

[2]For real and pseudoreal representations R the corresponding chiral symmetry group is $\mathrm{SU}(2N_\mathrm{F})$.

[3]If R is real, $\mathrm{SU}(2N_\mathrm{F})$ breaks down to $\mathrm{SO}(2N_\mathrm{F})$, and if R is pseudoreal, $\mathrm{SU}(2N_\mathrm{F})$ breaks down to $\mathrm{Sp}(2N_\mathrm{F})$.

[4]If R is real, the number of pions is $2N_\mathrm{F}^2 + N_\mathrm{F} - 1$, and if R is pseudoreal $2N_\mathrm{F}^2 - N_\mathrm{F} - 1$.

[5]Here τ_a are the generators of $\mathrm{SU}(2)$, and the field $q = \begin{pmatrix} u \\ d \end{pmatrix}$.

80.385 ± 0.015 GeV. In QCD these masses originate from processes that are shown diagrammatically in figure 1.1. Their effect is to shift the pole in the $W^{\pm}$ and Z^0 propagator away from zero.

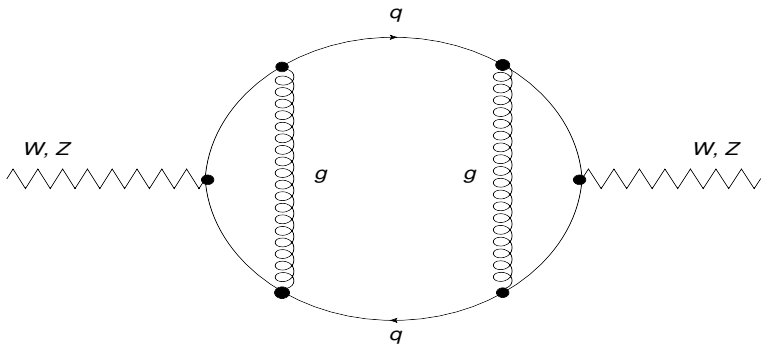

Figure 1.1: Typical QCD contribution to weak gauge boson vacuum polarization

Technicolor (TC) [8–11] is a theory that explains the EW symmetry breaking and the masses of the gauge bosons without a fundamental scalar field, thus avoiding the problems in its mathematical formulation. The idea is to introduce a new scaled up QCD-like interaction, where the equivalent of the QCD quark-antiquark condensate, the techniquark condensate $\langle \bar{Q}Q \rangle$, is much larger. To get the observed masses $\langle \bar{Q}Q \rangle$ has to be of the order 250 GeV at the TC scale Λ_{TC}. The Lagrangian of TC is

$$\mathcal{L}_{TC} = \bar{Q} \mathrm{i} D_\mu \gamma^\mu Q - \frac{1}{4} G^a_{\mu\nu} G^{\mu\nu}_a, \tag{1.29}$$

where the techniquark fields Q couple to TC, strong, weak and EM gauge fields through the covariant derivative D_μ and $G^a_{\mu\nu}$ is the field strength tensor for the TC gauge field.

In TC the techniquark condensate acts as a Higgs field, but it can not give masses to the fermions. For the fermion masses, the TC gauge group has to be extended so that the extended technicolor gauge group is spontaneously broken at a higher scale Λ_{ETC} and fermions and technifermions interact through this extended gauge interaction [12,13]. At low energy scales this interaction looks like a four fermion interaction. Schematic effective four fermion ETC interactions are of the form

$$\frac{g^2_{ETC}}{\Lambda^2_{ETC}} \bar{Q}Q\bar{Q}'Q', \quad \frac{g^2_{ETC}}{\Lambda^2_{ETC}} \bar{Q}Q\bar{q}q, \quad \frac{g^2_{ETC}}{\Lambda^2_{ETC}} \bar{q}q\bar{q}'q', \tag{1.30}$$

where g_{ETC} is the ETC coupling constant and Λ_{ETC} is the ETC scale. The fields q' and Q' represent (techni)quark fields that can have different flavors than q and Q. Writing this around the physical vacuum, where $\bar{Q}Q = \langle \bar{Q}Q \rangle + \bar{Q}_f Q_f$ and Q_f is the physical techniquark field fluctuation, we get terms proportional to operators

$$\langle \bar{Q}Q \rangle_{ETC} \bar{Q}_f Q_f, \quad \langle \bar{Q}Q \rangle_{ETC} \bar{q}q, \quad \bar{q}q\bar{q}'q', \quad \bar{Q}_f Q_f \bar{q}q, \quad \bar{Q}_f Q_f \bar{Q}'_f Q'_f, \tag{1.31}$$

where $\langle\bar{Q}Q\rangle_{ETC}$ is the value of techniquark condensate at the ETC scale. The first operator gives masses for the technipions. The second operator gives masses of the order

$$g_{ETC}^2\langle\bar{Q}Q\rangle_{ETC}\Lambda_{ETC}^{-2}, \tag{1.32}$$

to the SM fermions. The third and fourth operators in (1.31) generate flavor changing neutral currents through processes diagrammatically shown in figure 1.2. The last operator is uninteresting at the moment.

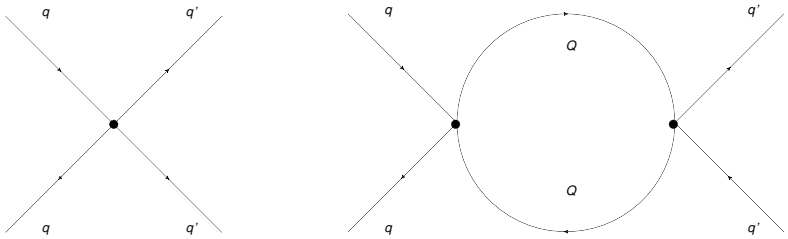

Figure 1.2: The processes that generate flavor changing neutral currents in ETC.

There are two problems with scaled-up QCD-like TC. First of all, TC should introduce a minimal number of new particles because particles not belonging to SM have not been observed. TC, with gauge group SU($N_{\rm TC}$), will always introduce technipions[6], from which three appear as longitudinal components of the weak gauge bosons. The masses of the remaining technipions have to be large enough that these particles would be too massive to appear in the experiments so far.

From the experimental data on $K^0 - \bar{K}^0$ mixing we get an upper limit for the scale Λ_{ETC} [14],

$$\Lambda_{ETC}^{-2} < 10^{-5}\ \text{TeV}^{-2}. \tag{1.33}$$

According to (1.32), we get $m_s \approx 0.1$ MeV for the strange quark, if we assume that $\langle\bar{Q}Q\rangle_{ETC} \approx \langle\bar{Q}Q\rangle_{TC}$ and $\Lambda_{ETC}/\Lambda_{TC} = 10^3$. This mass is roughly three orders of magnitude too small, which shows that the flavor changing neutral currents have to be somehow suppressed in order to get large enough fermion masses.

The renormalization group equation gives a way to calculate the scale dependence of the $\bar{Q}Q$ condensate. Because $m\bar{Q}Q$ is renormalization group invariant *i.e.* it is scale invariant, we get

$$\begin{aligned} & \frac{d}{d\mu}\left(m\bar{Q}Q\right) = 0 \\ \Rightarrow\quad & \frac{dm}{d\mu}\bar{Q}Q + m\frac{d\bar{Q}Q}{d\mu} = 0. \end{aligned} \tag{1.34}$$

[6]The number of technipions depends on $N_{\rm TC}$ and the fermionic representation R.

The anomalous dimension of the mass operator $\gamma = -\frac{d\log m}{d\log \mu} = -\frac{\mu}{m}\frac{dm}{d\mu}$ and so we get a first order differential equation for the scale dependence of $\bar{Q}Q$

$$-\frac{m\gamma}{\mu}\bar{Q}Q + m\frac{d\bar{Q}Q}{d\mu} = 0, \tag{1.35}$$

with a solution

$$\left(\bar{Q}Q\right)_{ETC} = \left(\bar{Q}Q\right)_{TC} \exp\left[\int_{\Lambda_{TC}}^{\Lambda_{ETC}} \frac{\gamma(\mu)}{\mu} d\mu\right]. \tag{1.36}$$

Theories in which the coupling stays nearly constant over a range of scales are called "walking" theories. For walking theories it is expected that the anomalous dimension of the mass operator $\gamma \approx 1$ [15]. Inserting $\gamma = 1$ to (1.36) we get

$$\left(\bar{Q}Q\right)_{ETC} = \left(\bar{Q}Q\right)_{TC} \frac{\Lambda_{ETC}}{\Lambda_{TC}}. \tag{1.37}$$

This enhances the $\bar{Q}Q$ condensate at the ETC scale by a factor of $\Lambda_{ETC}/\Lambda_{TC}$, which is enough to get realistic masses for the fermions [16, 17].

1.4 Running of the coupling

The coupling of the SU($N_{\rm C}$) theory runs as a function of the energy scale. It is usually quantified with the β-function, which is the derivative of the coupling as a function of the logarithm of the energy scale. For SU($N_{\rm C}$), ($N_{\rm C} > 1$), the β-function to two loops in perturbation theory is

$$\begin{aligned}
\beta(g) &\equiv \mu\frac{dg}{d\mu} = -\frac{\beta_0}{16\pi^2}g^3 - \frac{\beta_1}{(16\pi^2)^2}g^5, \\
\beta_0 &= \frac{11}{3}N_{\rm C} - \frac{4}{3}T(R)N_{\rm F}, \\
\beta_1 &= \frac{34}{3}N_{\rm C}^2 - \frac{20}{3}N_{\rm C}\,T(R)N_{\rm F} - 4C_2(R)T(R)N_{\rm F},
\end{aligned} \tag{1.38}$$

Above, $C_2(R)$ is the quadratic Casimir operator in representation R and $T(R)$ is defined for each representation as

$$\mathrm{Tr}(T^a T^b) = T(R)\delta^{ab}. \tag{1.39}$$

There are three different vacuum phases for SU($N_{\rm C}$) gauge theory, which can be classified with the β-function. For any $N_{\rm C}$ and small values of $N_{\rm F}$, the theories are QCD-like. This means that at low energy scales the coupling of the theory is large and it decreases as the energy scale is increased. The β-function and coupling as a function of a scale μ of such a theory is shown in figure 1.3.

The fact that the coupling constant behaves in this way has two implications. At large energies the fermions are asymptotically free and at small energies the fermions are bound to hadrons.

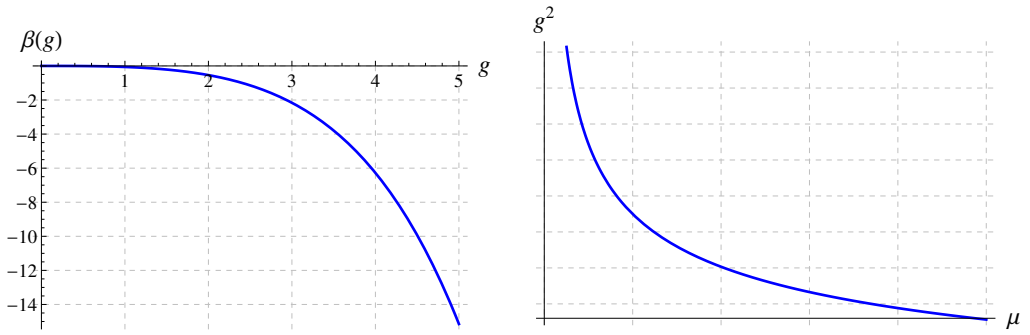

Figure 1.3: The β-function of QCD-like theory (left panel). Coupling constant of the corresponding theory as a function of logarithm of a scale μ (right panel).

If the number of fermionic flavors N_{F} is increased, the theory moves to a phase where the β-function is first negative and then goes through zero. A candidate for such a theory is SU(2) with 10 fundamental flavors. Its β-function to two loops in perturbation theory and the coupling as a function of scale μ is shown in figure 1.4. Such nontrivial zero in the β-function is called an infrared fixed point (IRFP).

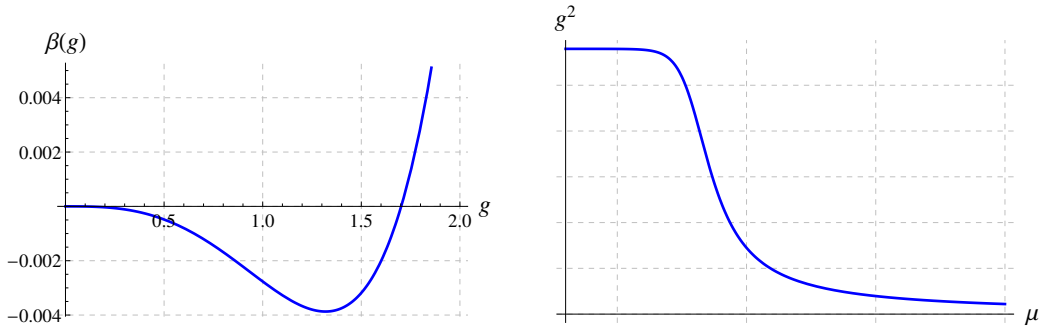

Figure 1.4: The β-function of SU(2) with $N_{\mathrm{F}} = 10$ fundamental fermions (left panel). Coupling constant of the theory as a function of logarithm of a scale μ (right panel).

When N_{F} is large enough asymptotic freedom is lost and the theory moves to a QED-like phase. In this phase the coupling is small in low energy scales and grows as the scale is increased. The β-function and coupling are shown in figure 1.5.

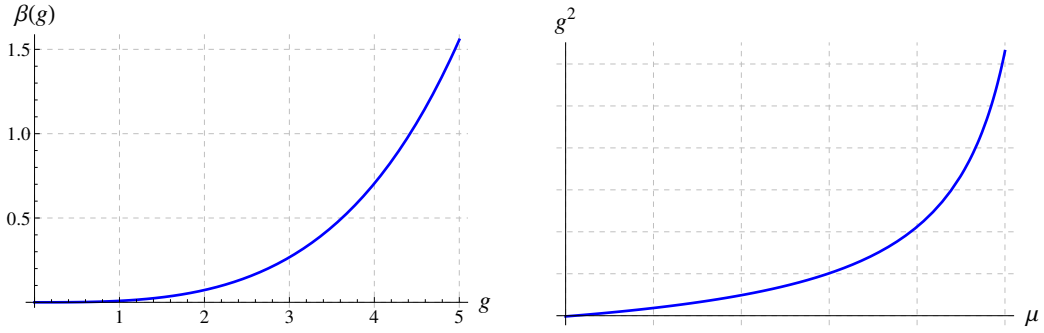

Figure 1.5: The β-function of QED-like theory (left panel). Coupling constant of the corresponding theory as a function of logarithm of a scale μ (right panel).

Between QCD-like and conformal phases there is a region, where theories show "walking" behavior. In these theories the coupling constant remains nearly constant over a range of scales. β-function and the coupling constant as a function of scale for such a theory is plotted in figure 1.6.

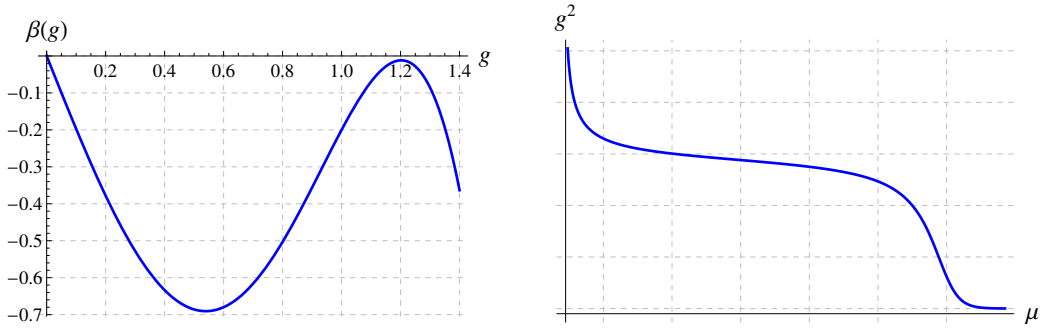

Figure 1.6: The β-function (left panel) and coupling constant (right panel) of a walking theory.

As stated earlier, theories that have a nontrivial IRFP or show walking dynamics are interesting for TC model building. Thus we want to estimate which theories could show such behavior. This can be done with perturbative tools. The upper limit for the number of flavors N_{F} for fixed N_{C} comes from the fact that the asymptotic freedom is lost when the one-loop coefficient β_0 of the β-function vanishes. At this point the theory moves from conformal phase to QED-like phase. For values of N_{F} that are smaller, the theory is expected to have a nontrivial IRFP. Near this upper boundary one expects the value of the coupling at the fixed point α^* to be small and perturbation theory to be applicable [18].

A theory can not be conformal if the chiral symmetry is broken, because the $\bar{q}q$ condensate introduces a scale in the system. Thus theories where chiral symmetry breaking is reached before the IRFP are not conformal. This gives us a lower limit to the conformal phase. The critical coupling for chiral symmetry

breaking in the ladder approximation is $\alpha_c = \pi/(3C_2(R))$ [19]. If we set α_c equal to the fixed point value of the two-loop coupling, which is

$$\alpha^* = -\frac{\beta_0}{\beta_1}(4\pi), \tag{1.40}$$

we obtain an approximation for the lower boundary of the conformal phase.

The area in $(N_{\rm C}, N_{\rm F})$-plane, where the conformal phase is possible according to the previous analysis, is called a conformal window. In figure 1.7 we show a sketch of SU($N_{\rm C}$) phase diagram in the $(N_{\rm C}, N_{\rm F})$-plane for fundamental, two-index (anti)symmetric and adjoint representations [20, 21]. The shaded regions in the figure depict the conformal windows for each of these fermion representations; below the conformal window the theory is in the chiral symmetry breaking and confining phase, while above the conformal window the theory is in the non-Abelian QED-like Coulomb phase.

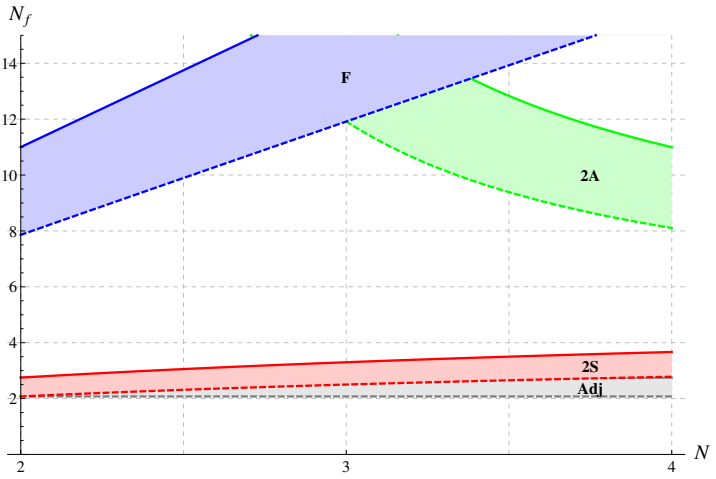

Figure 1.7: Phase diagram of SU($N_{\rm C}$) gauge theory as a function of the number of colors, flavors and fermion representations (F = Fundamental, 2A = 2-index antisymmetric, 2S = 2-index symmetric, Adj = Adjoint).

There are several recent studies of both SU(2) [22–33] and SU(3) [34–38] gauge theories with two-index symmetric representation fermions on the lattice. For studies of QCD-like theories with fundamental representation fermions see [III, 39–52].

1.5 Outline of the thesis

The main motivation for this work is TC related models, thus we are interested in gauge field theories that show (nearly) conformal behavior. The best tool that we have for studying strongly interacting theories is lattice simulations. However, distinguishing between two cases of slow running and conformal is

in no way a trivial task. To reliably do so, one must determine the coupling extremely accurately. In the second chapter we will explain in detail how one can remove some of the lattice artifacts that arise from the discretization of the continuum action.

Unfortunately, following the improvement procedure is not enough, if one wants to use higher representation fermions. In the third chapter we will show that large lattice effects appear if one naively implements higher representation fermions on the lattice and tries to measure the coupling. We will also provide a cure to remove these unwanted effects.

In the fourth chapter we will show results of SU(2) gauge theory simulations with $N_{\mathrm{F}} = 4$, 6 and 10 fundamental fermions, where we have implemented these improvements.

Chapter 2

Wilson action, Schrödinger functional and $\mathcal{O}(a)$ improvement

In this chapter we will present the lattice action that has been used throughout this work. We will also show the need for the improved actions that arise from the Wilson fermions and the Schrödinger functional boundary conditions. Finally, we will present all the necessary counter terms which cancel all linear contributions in the lattice spacing a from the action. After this improvement the results converge more rapidly to the continuum limit.

2.1 Wilson action

The Wilson lattice action was first proposed by Wilson in [53]. It can be divided into a gauge part S_{G} and a fermionic part S_{F}

$$S_0 = S_{\mathrm{G}} + S_{\mathrm{F}}. \tag{2.1}$$

Here the standard Wilson plaquette action is

$$S_{\mathrm{G}} = \beta_L \sum_{x;\mu<\nu} \left(1 - \frac{1}{N}\mathrm{Re}\big[\mathrm{Tr}[U_\mu(x)U_\nu(x+a\hat{\mu})U_\mu^\dagger(x+a\hat{\nu})U_\nu^\dagger(x)]\big]\right), \tag{2.2}$$

with $\beta_L = 2N/g_0^2$, and the link matrices

$$U_\mu(x) = \exp(\mathrm{i}ag_0A_\mu(x)). \tag{2.3}$$

If S_{G} is expanded with respect to the lattice coupling a,

$$S_{\mathrm{G}} = \frac{\beta_L}{4}a^4\sum_x F_{\mu\nu}(x)F^{\mu\nu}(x) + \mathcal{O}(a^6). \tag{2.4}$$

From equation (2.4) we can see that when the lattice spacing a is taken to zero, the gauge part of the action converges to the continuum gauge action and the next terms in the series vanish as a^2.

The Wilson fermion action, $S_{\rm F}$, for $N_{\rm F}$ (mass degenerate) Dirac fermions is

$$S_{\rm F} = a^4 \sum_x \bar{\psi}(x)(D_0 + m_{q,0}\mathbb{1})\psi(x), \tag{2.5}$$

where the unimproved Wilson-Dirac operator is

$$D_0 = \frac{1}{2}(\gamma_\mu(\nabla^*_\mu + \nabla_\mu) - a\nabla^*_\mu\nabla_\mu). \tag{2.6}$$

This involves the gauge covariant lattice derivatives ∇_μ and ∇^*_μ defined as

$$\begin{aligned} \nabla_\mu\psi(x) &= \frac{1}{a}[\widetilde{U}_\mu(x)\psi(x+a\hat{\mu}) - \psi(x)], & (2.7)\\ \nabla^*_\mu\psi(x) &= \frac{1}{a}[\psi(x) - \widetilde{U}^{-1}_\mu(x-a\hat{\mu})\psi(x-a\hat{\mu})], & (2.8) \end{aligned}$$

where $\widetilde{U}$ is the parallel transporter in the appropriate fermion representation.

If we want our action to be free of $\mathcal{O}(a)$ terms and thus converge quadratically to the continuum limit, we must add new terms to the action so that the linear contributions cancel. These counter terms were first studied by Sheikholeslami and Wohlert in [54]. It turns out that it is sufficient to add just one new term

$$\begin{aligned} S_{\rm impr} &= S_0 + \delta S_{\rm sw}, & (2.9)\\ \delta S_{\rm sw} &= a^5 \sum_x c_{\rm sw}\bar{\psi}(x)\frac{\rm i}{4}\sigma_{\mu\nu}F_{\mu\nu}(x)\psi(x), & (2.10) \end{aligned}$$

to cancel $\mathcal{O}(a)$ from all on-shell quantities as long as the coefficient $c_{\rm sw}$ is chosen correctly. In equations (2.10) and (2.12) $\sigma_{\mu\nu} = i[\gamma_\mu, \gamma_\nu]/2$ and $F_{\mu\nu}(x)$ is the symmetrized lattice field strength tensor. Now we can write our improved fermionic action as

$$S_{\rm F,impr} = a^4 \sum_x \bar{\psi}(x)(D + m_{q,0}\mathbb{1})\psi(x), \tag{2.11}$$

where the Wilson-Dirac operator is

$$D = \frac{1}{2}[\gamma_\mu(\nabla^*_\mu + \nabla_\mu) - a\nabla^*_\mu\nabla_\mu] + c_{\rm sw}\frac{{\rm i}a}{4}\sigma_{\mu\nu}F_{\mu\nu}(x). \tag{2.12}$$

This improvement coefficient can be determined perturbatively [55,56] and non-perturbatively [I,57] and to the lowest order in perturbation theory $c_{\rm sw} = 1$ [54].

The boundary values of the fermion fields are set as

$$\begin{aligned} P_+\psi(x_0 = 0, \mathbf{x}) &= \rho(\mathbf{x}), \;\; P_-\psi(x_0 = T, \mathbf{x}) = \rho'(\mathbf{x}),\\ P_-\psi(x_0 = 0, \mathbf{x}) &= P_+\psi(x_0 = T, \mathbf{x}) = 0, \end{aligned} \tag{2.13}$$

with similar definitions on the conjugate fields. The projection operators are $P_\pm = \frac{1}{2}(1 \pm \gamma_0)$. The boundary fields ρ, ρ' are source fields for correlation functions, and they are set to zero when generating configurations in simulations.

In the spatial directions it is customary to introduce a "twist" for the phase of the fermion fields [58]:

$$\psi(x + L\hat{k}) = e^{\mathrm{i}\theta_k}\psi(x), \;\; \bar{\psi}(x + L\hat{k}) = \bar{\psi}(x)e^{-\mathrm{i}\theta_k}. \tag{2.14}$$

This is done to maximize the smallest eigenvalue of the Dirac operator. In this work we use $\theta_k = \pi/5$ throughout, which is optimal for fundamental fermions[1]. The twist, together with the Dirichlet boundary conditions, regulates the fermion matrix so that simulations at zero fermion masses become possible.

With perturbative calculations, one must also fix the gauge. This will add two new terms to the action S_{GF} and S_{FP}. The specific form of these terms is only important while calculating the contribution of the gauge sector to observables. Since we will mainly be focused on the fermionic contribution, we refer the interested reader to the original article [60].

2.2 Schrödinger functional

Measurements of the coupling constant on the lattice are usually done using the Schrödinger functional. It is an effective tool to study the scaling properties of the coupling constant on the lattice. Basically we introduce a constant background field to the space-time by setting boundary conditions for the gauge fields on times $T = 0$ and $T = L$. In the spatial directions we apply periodic boundary conditions for the gauge field, thus the space-time is a cylinder. We can then study how the coupling responds to changes in the background field.

The boundary fields used throughout this thesis for SU(2) are

$$C_k = \frac{\mathrm{i}}{L}\begin{pmatrix} \phi_1 & 0 \\ 0 & \phi_2 \end{pmatrix}, \qquad C'_k = \frac{\mathrm{i}}{L}\begin{pmatrix} \phi'_1 & 0 \\ 0 & \phi'_2 \end{pmatrix}, \quad k = 1, 2, 3, \tag{2.15}$$

where

$$\begin{array}{lcllcl} \phi_1 &=& -\eta, & \phi'_1 &=& \eta - \rho, \\ \phi_2 &=& \eta, & \phi'_2 &=& \rho - \eta. \end{array} \tag{2.16}$$

The standard choice for the angles are $\eta = \frac{\pi}{4}$ and $\rho = \pi$. For SU(3) we use

$$C_k = \frac{\mathrm{i}}{L}\begin{pmatrix} \phi_1 & 0 & 0 \\ 0 & \phi_2 & 0 \\ 0 & 0 & \phi_3 \end{pmatrix}, \qquad C'_k = \frac{\mathrm{i}}{L}\begin{pmatrix} \phi'_1 & 0 & 0 \\ 0 & \phi'_2 & 0 \\ 0 & 0 & \phi'_3 \end{pmatrix}, \quad k = 1, 2, 3, \tag{2.17}$$

where

$$\begin{array}{lcllcl} \phi_1 &=& \eta - \rho, & \phi'_1 &=& -\phi_1 - 4\rho, \\ \phi_2 &=& \eta(\nu - \frac{1}{2}), & \phi'_2 &=& -\phi_3 + 2\rho, \\ \phi_3 &=& -\eta(\nu + \frac{1}{2}) + \rho, & \phi'_3 &=& -\phi_2 + 2\rho. \end{array} \tag{2.18}$$

The standard choice for the angles are $\eta = 0$, $\rho = \frac{\pi}{3}$ and $\nu = 0$.

[1] For optimal choice of θ_k for other representations see [59].

When one uses fermions in a higher representation these boundary fields have to be transformed to the corresponding representation. For the adjoint representation the transformation is

$$C_k(\mathrm{adj})_{ab} = 2\mathrm{Tr}(T^a C_k(\mathrm{F}) T^b C_k(\mathrm{F})^\dagger), \tag{2.19}$$

where $T^a = \sigma^a/2$ are the generators of the fundamental representation. This also works for C'_k. For the (anti)symmetric representation the transformation is

$$C_k((\mathrm{a})\mathrm{s})_{ab} = \pm\mathrm{Tr}(K^a C_k(\mathrm{F}) K^b C_k(\mathrm{F})), \tag{2.20}$$

where the upper (lower) sign refers to the (anti)symmetric representation and the matrices K^a form a basis in the space of (anti)symmetric $N \times N$ matrices. After the transformation one has to diagonalize the resulting matrix in order to get the right boundary field.

With the boundary matrices C_k and C'_k from (2.15), (2.17), (2.16) and (2.18) we end up with a background field of the form

$$B_0 = 0, \qquad B_k = (x_0 C'_k + (L - x_0)C_k)/L, \quad k = 1, 2, 3. \tag{2.21}$$

The path integral representation of the Schrödinger functional is

$$\mathcal{Z}(C, C') = \int D(\psi) D(\bar{\psi}) D(U) D(c) D(\bar{c}) \exp(-S) \tag{2.22}$$

This can also be written as an effective action

$$\Gamma = -\ln \mathcal{Z}, \tag{2.23}$$

which has the perturbative expansion of the form

$$\Gamma = g_0^{-2}\Gamma_0 + \Gamma_1 + \mathcal{O}(g_0^2). \tag{2.24}$$

The effective action can be used to define the running coupling

$$\bar{g}^2(L) = \frac{\partial\Gamma_0/\partial\eta}{\partial\Gamma/\partial\eta}. \tag{2.25}$$

This gives us a way to calculate the running coupling perturbatively

$$\begin{aligned} \bar{g}^2(L) &= \frac{\partial\Gamma_0/\partial\eta}{\partial(g_0^{-2}\Gamma_0 + \Gamma_1)/\partial\eta}, \\ &= g_0^2 + p_1(L) g_0^4 + \mathcal{O}(g_0^6), \end{aligned} \tag{2.26}$$

where

$$p_1(L) = -\frac{\partial\Gamma_1/\partial\eta}{\partial\Gamma_0/\partial\eta}. \tag{2.27}$$

This quantity will be important in the calculation of one of the improvement coefficients and the step scaling function.

The fixed boundary conditions at times $t = 0$ and $t = T$ will again introduce $\mathcal{O}(a)$ errors to the action. Removal of these errors has first been studied in [56, 60, 61]. There it has been shown that the necessary counter terms are

$$\begin{aligned}
\delta S_V &= \frac{\mathrm{i}a^5}{4} c_{\mathrm{sw}} \sum_{x_0=a}^{L-a} \sum_{\vec{x}} \bar{\psi}(x) \sigma_{\mu\nu} \hat{F}_{\mu\nu}(x) \psi(x), && (2.28)\\
\delta S_{G,b} &= \frac{1}{2g_0^2}(c_s - 1) \sum_{p_s} \mathrm{Tr}[1 - U(p_s)] \\
&\quad + \frac{1}{g_0^2}(c_t - 1) \sum_{p_t} \mathrm{Tr}[1 - U(p_t)], && (2.29)\\
\delta S_{F,b} &= a^4(\tilde{c}_s - 1) \sum_{\vec{x}} [\hat{O}_s(\vec{x}) + \hat{O}'_s(\vec{x})] \\
&\quad + a^4(\tilde{c}_t - 1) \sum_{\vec{x}} [\hat{O}_t(\vec{x}) - \hat{O}'_t(\vec{x})]. && (2.30)
\end{aligned}$$

Here we have introduced the operators

$$\begin{aligned}
\hat{O}_s(\vec{x}) &= \frac{1}{2} \bar{\psi}(0, \vec{x}) P_- \gamma_k (\nabla_k^* + \nabla_k) P_+ \psi(0, \vec{x}), && (2.31)\\
\hat{O}'_s(\vec{x}) &= \frac{1}{2} \bar{\psi}(L, \vec{x}) P_+ \gamma_k (\nabla_k^* + \nabla_k) P_- \psi(L, \vec{x}), && (2.32)\\
\hat{O}_t(\vec{x}) &= \left\{ \bar{\psi}(y) P_+ \nabla_0^* \psi(y) + \bar{\psi}(y) \overleftarrow{\nabla}_0^* P_- \psi(y) \right\}_{y=(a,\vec{x})}, && (2.33)\\
\hat{O}'_t(\vec{x}) &= \left\{ \bar{\psi}(y) P_- \nabla_0 \psi(y) + \bar{\psi}(y) \overleftarrow{\nabla}_0 P_+ \psi(y) \right\}_{y=(T-a,\vec{x})}. && (2.34)
\end{aligned}$$

By tuning the coefficients $c_{\mathrm{sw}}, c_s, c_t, \tilde{c}_s, \tilde{c}_t$ to their proper values we can remove all the $\mathcal{O}(a)$ errors.

For the electric background fields which we consider, the terms proportional to c_s do not contribute. Also, if we set the fermionic fields to zero on the boundaries, the counter term proportional to $\tilde{c}_s$ vanishes. However the two terms proportional to c_t and $\tilde{c}_t$ remain nonzero. The $\tilde{c}_t$ term corrects the mass of the fermions at times $T = a$ and $T = L - a$ and the c_t term changes the weight of the time-like plaquettes on the boundary.

2.3 Perturbative analysis of the boundary improvement

All boundary coefficients have a perturbative expansion of the form

$$c_x = 1 + c_x^{(1)} g_0^2 + \mathcal{O}(g_0^4). \tag{2.35}$$

Next we will determine the coefficients $\tilde{c}_t$ and c_t to one-loop order in perturbation theory for different gauge groups and fermionic representations.

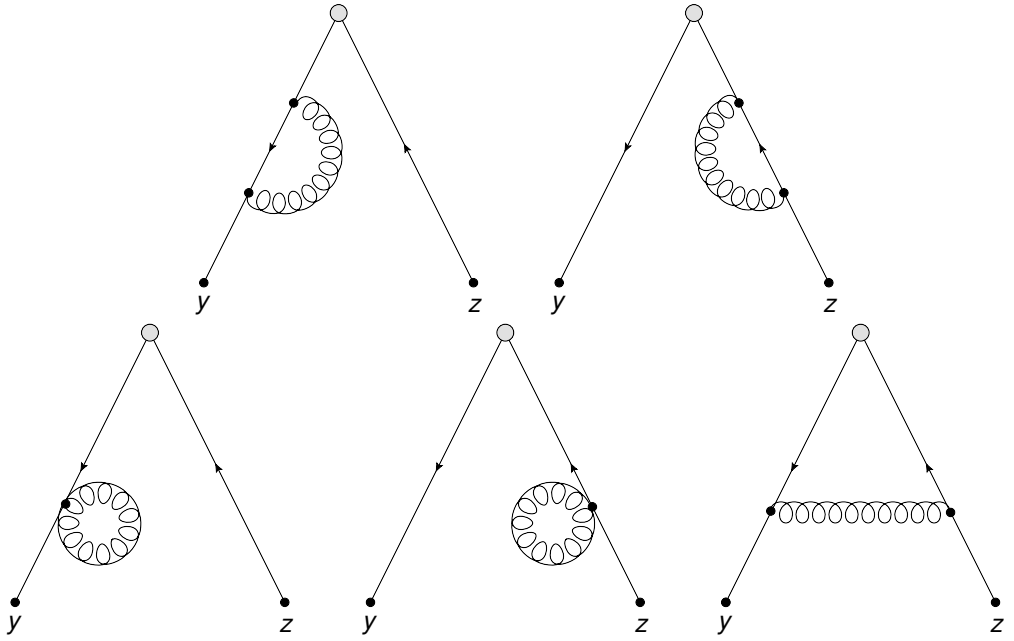

Figure 2.1: Diagrams contributing to the calculation of $\tilde{c}_t^{(1)}$. The shaded blobs indicate insertion of operator $\Gamma_x = \{\mathbb{1}, \gamma_5\}$.

Coefficient $\tilde{c}_t^{(1)}$

The coefficient $\tilde{c}_t$ was first calculated in [56] for fermions in the fundamental representation. The result of [56] is

$$\tilde{c}_t^{(1)} = -0.0135(1)C_F, \tag{2.36}$$

and this generalizes to other fermion representations simply by replacing the fundamental representation Casimir operator C_F with Casimir operator C_R of the representation R under consideration. This is so because the relevant correlation functions are proportional to the diagrams presented in figure 2.1, which all include the color factor $\sum_a (T^a)^2 = C_R$. Thus it can be shown that $\tilde{c}_t^{(1)} \propto C_R$. The results for gauge groups SU(2) and SU(3) and different fermion representations are shown in table 2.1.

Coefficient $c_t^{(1)}$

The coefficient $c_t^{(1)}$ can be split into gauge and fermionic parts

$$c_t^{(1)} = c_t^{(1,0)} + c_t^{(1,1)} N_{\mathrm{F}}. \tag{2.37}$$

The contribution $c_t^{(1,0)}$ is entirely due to gauge fields and has been evaluated in [60] for SU(2) and in [62] for SU(3). The fermionic contribution $c_t^{(1,1)}$ to c_t has been evaluated for fundamental fermions in [63], both for SU(2) and SU(3). We

have extended these computations for SU(2) and SU(3) gauge theory with higher representation fermions. The results for the nonzero improvement coefficients are shown in table 2.1. The numbers beyond the fundamental representation are new, while those for the fundamental representation provide a good check on our computations.

The idea behind the calculation of $c_t^{(1,1)}$ is to find an observable whose $\mathcal{O}(a)$ contribution to one loop order in perturbation theory is only sensitive to the boundary counter term c_t. One suitable observable turns out to be p_1, which was introduced in equation (2.27). The method was developed and applied first for the pure gauge theory case in [60], and later for fundamental representation fermions in [63].

In p_1 the tree level contribution

$$\Gamma_0 = g_0^2 S_{\mathrm{G}}(B) = L^4 \sum_{k=1}^{3} \sum_{i=1}^{N} \left\{ \frac{2}{a^2} \sin\left[\frac{a^2}{2L^2}(\phi_i' - \phi_i) \right] \right\}, \tag{2.38}$$

is just the gauge part of the action calculated at the generated background field B. The value of the normalizing factor in p_1 is then

$$k = \frac{24L^2}{a^2} \left\{ \sin\left[\frac{a^2}{L^2}(\pi - 2\eta) \right] \right\} \tag{2.39}$$

for SU(2) and

$$k = \frac{\partial \Gamma_0}{\partial \eta} = \frac{12L^2}{a^2} \left\{ \sin\left[\frac{2a^2}{3L^2}(3\eta + \pi) \right] + \sin\left[\frac{a^2}{3L^2}(3\eta + \pi) \right] \right\} \tag{2.40}$$

for SU(3). The value of the normalizing factor k does not change when one uses higher representation fermions.

The nominator in (2.27) can be written in terms of lattice operators via

$$\Gamma_1 = \frac{1}{2} \ln\det \Delta_1 - \ln\det \Delta_0 - \frac{1}{2} \ln\det \Delta_2 \tag{2.41}$$

where the first two terms are due to the gauge part and the ghost part of the action, and the last term comes from the fermionic part. Their contributions can also be split into gauge and fermionic parts

$$p_1 = p_{1,0} + N_{\mathrm{F}} p_{1,1} = -\frac{1}{k} \left(\frac{1}{2} \ln\det \Delta_1 - \ln\det \Delta_0 \right) + \frac{N_{\mathrm{F}}}{k} \left(\frac{1}{2} \ln\det \Delta_2 \right). \tag{2.42}$$

The operators Δ_0, Δ_1 and Δ_2 can be expressed in terms of the lattice variables. However the definitions of Δ_0 and Δ_1 are related to the S_{GF} and S_{FP} parts of the action which we did not define, thus the expressions of these operators will not be presented here. We again refer the reader to the original article [60]. The last operator has a simple form

$$\Delta_2 = [(D + m_0)\gamma_5]^2, \tag{2.43}$$

where D is the lattice Dirac-Wilson operator defined in (2.12) and $\gamma_5 = \gamma_0\gamma_1\gamma_2\gamma_3$.

To calculate p_1 one then has to determine the determinants of the three operators Δ_0, Δ_1 and Δ_2. It can be shown that eigenvalue equations of these operators have equivalent recursion relations. Subsequently one simply has to solve these recursion relations to get the eigenvalues, and the determinant is then the product of these eigenvalues. Using this method p_1 can be calculated for a range of values of L. We know that $p_{1,0}$ and $p_{1,1}$ can be in the large L limit expanded as

$$p_{1,x} \sim \sum_{n=0}^{\infty} (r_n + s_n \ln L)/L^n, \qquad x = 0, 1, \tag{2.44}$$

where $s_0 = 2b_{0,x}$, $r_1 = 2c_t^{(1,x)}$ and $s_1 = 0$. The coefficient $b_{0,x}$ refers to the one loop beta function

$$b_0 = b_{0,0} + N_{\mathrm{F}} b_{0,1} = \frac{1}{(4\pi)^2}\left(\frac{11N}{3} - \frac{4T_{\mathrm{R}}N_{\mathrm{F}}}{3}\right), \tag{2.45}$$

where T_{R} is the normalization of the representation R, defined as $\mathrm{Tr}(T_R^a T_R^b) = T_{\mathrm{R}}\delta^{ab}$. The main task now is to fit $p_{1,x}$ data using (2.44) to extract the value of r_1. This then gives $c_t^{(1,x)}$. We have used the blocking transformation from [64].

Our results are consistent with the generic formula

$$c_t^{(1,1)} \approx 0.019141(2T_{\mathrm{R}}). \tag{2.46}$$

We have also plotted our results of $c_t^{(1,1)}$ scaled with $1/(2T_{\mathrm{R}})$ against (2.46) in

N_{C}	rep.	$c_t^{(1,0)}$	$c_t^{(1,1)}$	$\tilde{c}_t^{(1)}$
2	**2**	−0.0543(5)	0.01914(2)	−0.0101(3)
2	**3**	−0.0543(5)	0.0766(2)	−0.0270(2)
3	**3**	−0.08900(5)	0.01914(6)	−0.0180(1)
3	**8**	−0.08900(5)	0.1148(3)	−0.0405(3)
3	**6**	−0.08900(5)	0.0957(2)	−0.0450(3)

Table 2.1: The nonzero improvement coefficients for Schrödinger functional boundary conditions with electric background field for various gauge groups and fermion representations.

figure 2.2. Although we were unable to achieve the accuracy of the original work [63], our results are fully compatible for fundamental representation fermions. The figure also clearly indicates that $c_t^{(1,1)}$ scales with $2T_{\mathrm{R}}$.

Now we have shown that all $\mathcal{O}(a)$ terms can be canceled from the action by introducing the proper counter terms and tuning the corresponding improvement coefficients. Unfortunately this is not enough. In the next chapter we will show that even after the improvement, the discretization errors can be large if the boundary conditions are chosen poorly.

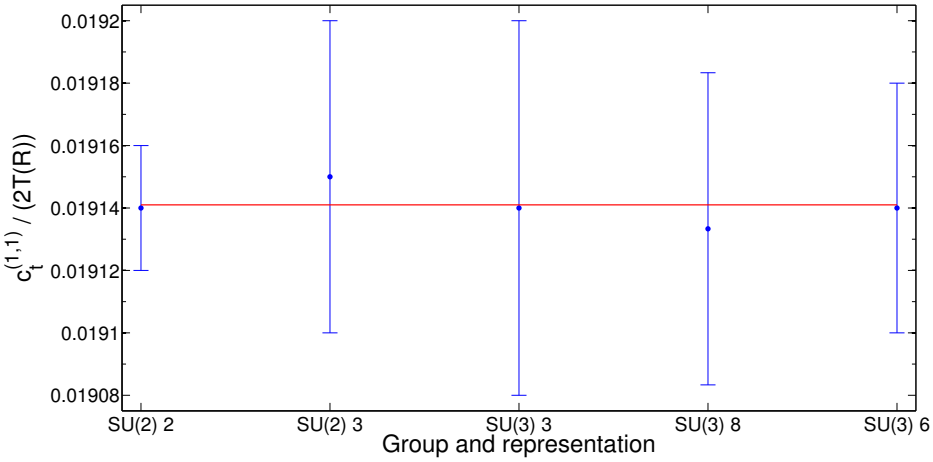

Figure 2.2: Our results of $c_t^{(1,1)}$ scaled with $2T_{\mathrm{R}}$ (blue dots with errorbars) compared with conjectured value of $c_t^{(1,1)}/(2T_{\mathrm{R}})$ (red line).

Chapter 3

Perturbative analysis of the boundary conditions

In this chapter we will introduce the step scaling function, and compute it to one loop order in perturbation theory. The main observation is that the Schrödinger functional boundary conditions can introduce large higher order errors in lattice spacing a, if the boundary fields are not chosen correctly.

3.1 Step scaling

There is a growing interest in the scaling properties of the coupling constant in gauge theories with fermions in higher representations. Many research groups use the step scaling function to measure the running of the coupling. The step scaling function and its perturbative expansion to one loop are

$$\begin{aligned} \Sigma(u, s, L/a) &= g^2(g_0, sL/a)|_{g^2(g_0, L/a)=u}, & (3.1)\\ &= u + [\Sigma_{1,0}(s, L/a) + \Sigma_{1,1}(s, L/a)N_{\mathrm{F}}]\, u^2 + \mathcal{O}(u^3). & (3.2) \end{aligned}$$

Using the perturbative expansion of the coupling from (2.26) in the perturbative formula for the step scaling function, we obtain for the one loop coefficients the following useful formulas:

$$\begin{aligned} \Sigma_{1,0}(s, L/a) &= p_{1,0}(sL) - p_{1,0}(L), & (3.3)\\ \Sigma_{1,1}(s, L/a) &= p_{1,1}(sL) - p_{1,1}(L). & (3.4) \end{aligned}$$

We also introduce the variable

$$\delta_i = \frac{\Sigma_{1,i}(2, L/a)}{\sigma_{1,i}(2)} = \frac{\Sigma_{1,i}(2, L/a)}{2b_{0,i}\ln 2}, \qquad i = 0, 1, \tag{3.5}$$

which is the ratio of the perturbative step scaling and its continuum limit. This variable is useful in illustrating the convergence of the step scaling. In equation (3.5) we used

$$b_{0,0} = 11N_{\mathrm{C}}/(48\pi^2), \qquad b_{0,1} = T_{\mathrm{R}}/(12\pi^2), \tag{3.6}$$

which are the one loop coefficients of the perturbative beta function.

It has been shown in [63, 65] that for SU(2) and SU(3) with fundamental fermions $\Sigma_{1,1}(s, L/a)$ converges rapidly to its continuum limit when one uses improved action. This can also easily be seen in the left panel of figure 3.1. However, the situation changes when one considers fermions in the higher representations, which can be seen from the right panel of figure 3.1.

Clearly the fermionic step scaling function for the higher representations has large $\mathcal{O}(a^2)$ contributions, which are absent in the step scaling for the fundamental representation fermions. In the following we will study the effect of the Schrödinger functional boundary conditions on the convergence of step scaling. In [66] these errors are removed from SU(3) with sextet fermions by decreasing the boundary fields by a factor 2.

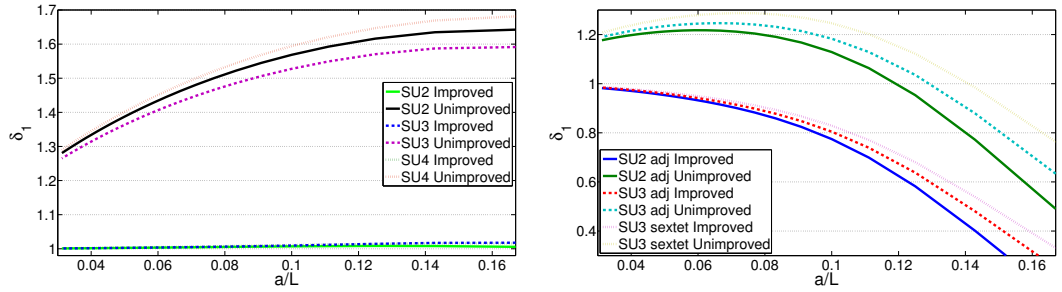

Figure 3.1: Fermionic parts of the Lattice step scaling function with fundamental (left) and higher representation (right) fermions.

3.2 Fundamental domain

The choice of the boundary fields in (2.16) and (2.18) is in no way unique. In fact one can choose the form of the boundary fields and the values of the angles η, ρ and ν quite freely. The only limitation is that the fields ϕ and ϕ' have to belong to the so called fundamental domain. This consists of all the boundary fields that satisfy the equations

$$\phi_1 < \phi_2 < \ldots < \phi_n, \qquad |\phi_i - \phi_j| < 2\pi, \text{for all } i, j, \qquad \sum_{i=1}^{N} \phi_i = 0. \quad (3.7)$$

Boundary fields of this type lead to a unique (up to a gauge transformation) minimal action, as shown in [60].

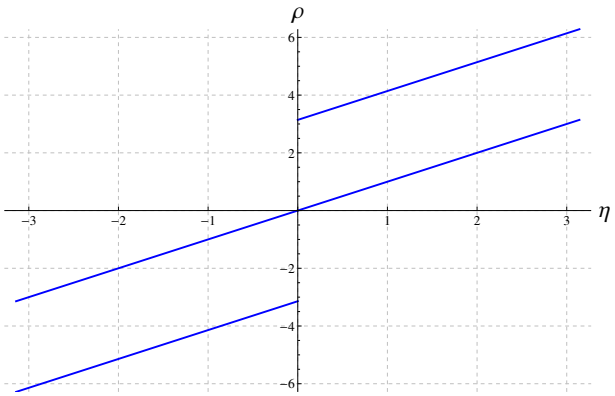

Figure 3.2: The fundamental domain for SU(2) with the parametrization for the boundary fields chosen as in (3.8).

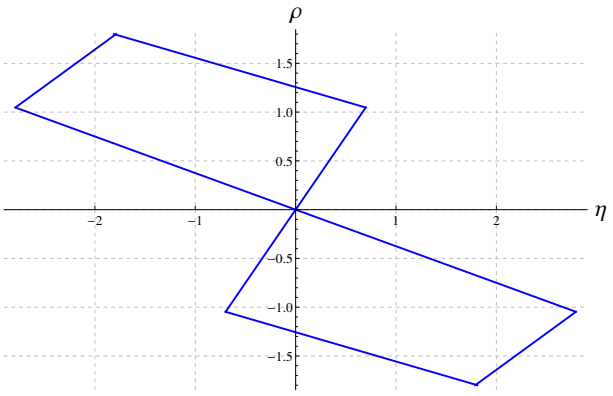

Figure 3.3: The fundamental domain for SU(3) with the parametrization for the boundary fields chosen as in (3.9).

We take the fields ϕ and ϕ' that were introduced in equations (2.16) and (2.18), set $\nu = 0$, and choose variables η and ρ to be free parameters. The equation (3.7) then gives us the range of allowed values for η and ρ[1]. For SU(2) we get

$$\eta \in]0, \pi[, \;\; \rho \in]\eta, \pi + \eta[, \quad \text{and} \quad \eta \in]-\pi, 0[, \;\; \rho \in]-\pi + \eta, \eta[. \tag{3.8}$$

[1]We drop the requirement in (3.7) that $\phi_1 < \phi_2 \ldots \phi_n$, since the angles ϕ_i can be reordered after the choice of η and ρ.

These areas are presented in figure 3.2. For SU(3) the fundamental domain is

$$\begin{aligned}
\eta \in]-\tfrac{8\pi}{9}, -\tfrac{4\pi}{7}],\ \rho \in]-\tfrac{3\eta}{8}, \tfrac{4\pi+3\eta}{4}[\cup \\
\eta \in]-\tfrac{4\pi}{7}, 0],\ \rho \in]-\tfrac{3\eta}{8}, \tfrac{4\pi-3\eta}{10}[\cup \\
\eta \in]0, \tfrac{2\pi}{9}[,\ \rho \in]\tfrac{3\eta}{2}, \tfrac{4\pi-3\eta}{10}[,
\end{aligned}$$

and

$$\begin{aligned}
\eta \in]-\tfrac{2\pi}{9}, 0],\ \rho \in]-\tfrac{4\pi+3\eta}{10}, \tfrac{3\eta}{2}[\cup \\
\eta \in]0, \tfrac{4\pi}{7}],\ \rho \in]-\tfrac{4\pi+3\eta}{10}, -\tfrac{3\eta}{8}[\cup \\
\eta \in]\tfrac{4\pi}{7}, \tfrac{8\pi}{9}[,\ \rho \in]\tfrac{-4\pi+3\eta}{4}, -\tfrac{3\eta}{8}[,
\end{aligned} \tag{3.9}$$

and it is presented in figure 3.3. The boundary fields that the latter areas produce are in both cases equivalent to the boundary fields of the former area and thus we only need to scan half of the parameter space. Now we can study δ_i at fixed L as a function of η and ρ as we let these variables range over the values belonging to the fundamental domain. This in turn will allow us to determine the background field for which the step scaling function converges most rapidly.

3.3 Higher representations

From now on we will use the terms "old" and "new" boundary conditions. The old boundary conditions refer to the conditions presented in equations (2.16) and (2.18) with the standard choice of parameters ρ and η. With the term new boundary conditions we refer to the optimal choice of the parameters ρ and η for a specific symmetry group and fermion representation as stated in this chapter.

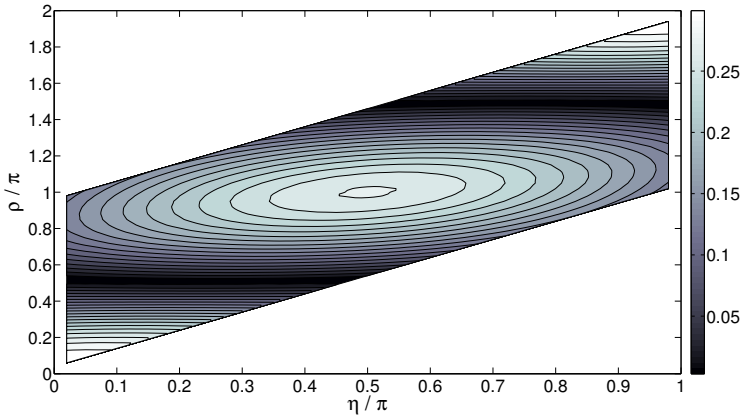

Figure 3.4: Convergence of $|\delta_1 - 1|$ as a function of η/π and ρ/π for SU(2) with adjoint fermions at $L = 10$. The optimal choice is $\rho = \frac{\pi}{2}$ and $\eta = \frac{\pi}{8}$.

We consider first SU(2) with two adjoint Dirac fermions. There are two darker regions in figure 3.4, indicating the areas where the discretization errors

are smallest. These two values of ρ, $\pi/2$ and $3\pi/2$ are actually equivalent. The η dependence is weak, and η can be selected from the values within the fundamental domain quite freely (this turns out to also be true for SU(3)). However, the value $\eta = \rho/2$ must be excluded, since the step scaling function diverges at that point.

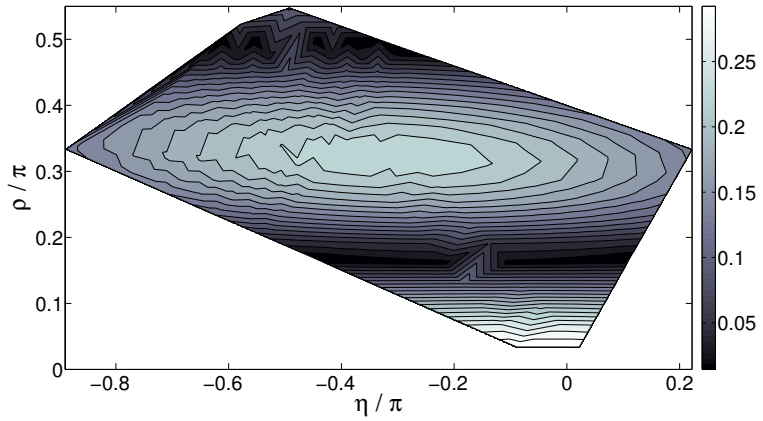

Figure 3.5: Convergence of $|\delta_1 - 1|$ as a function of η/π and ρ/π for SU(3) with adjoint fermions at $L = 10$. The optimal choice is $\rho = \frac{\pi}{6}$ and $\eta = -\frac{\pi}{9}$.

We then turn to SU(3) with two Dirac fermions either in the adjoint or the sextet representation. Figure 3.5 also shows two darker areas for SU(3) with adjoint fermions. More detailed analysis shows that in the $\rho = \pi/6$ area the $\mathcal{O}(a^2)$ effects are smaller. In figure 3.6, which shows the step scaling function for SU(3) sextet, there is only one dark region at $\rho = 67\pi/150$. We also found that these optimal values of η and ρ are independent of L. A change in L only modifies the scale of the errors.

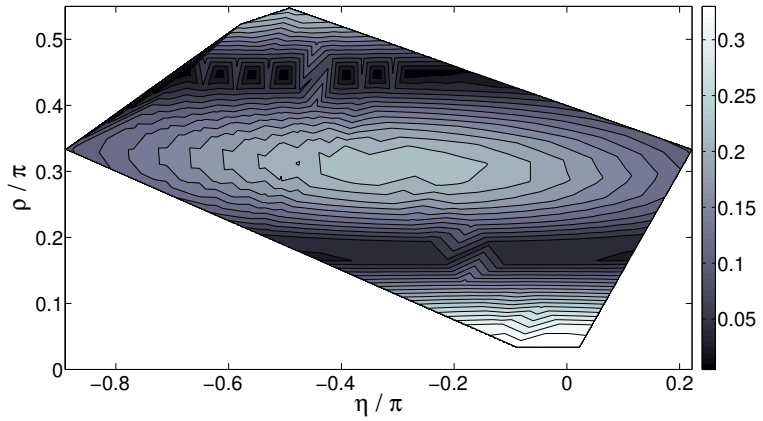

Figure 3.6: Convergence of $|\delta_1 - 1|$ as a function of η/π and ρ/π for SU(3) with sextet fermions at $L = 10$. The optimal choice is $\rho = \frac{67\pi}{150}$ and $\eta = -\frac{\pi}{3}$.

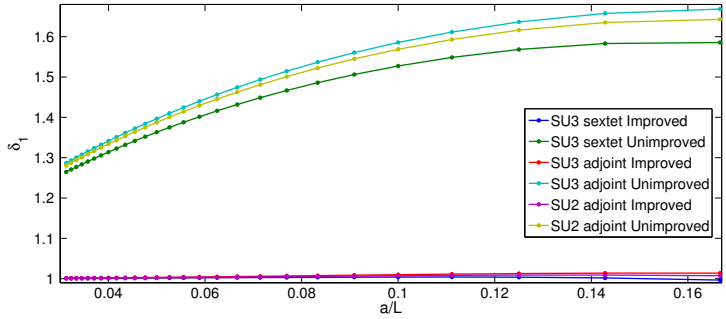

Figure 3.7: Fermionic part of the Lattice step scaling function for higher representation fermions with the new boundary conditions.

We also want to be sure that the value of the step scaling parameter s does not have an effect on the preferred values of angles η and ρ. Thus we have also done similar contour plots for a range of s values. These are presented in figure 3.8. These figures clearly show that the convergence of the step scaling as a function of η and ρ does not depend on s.

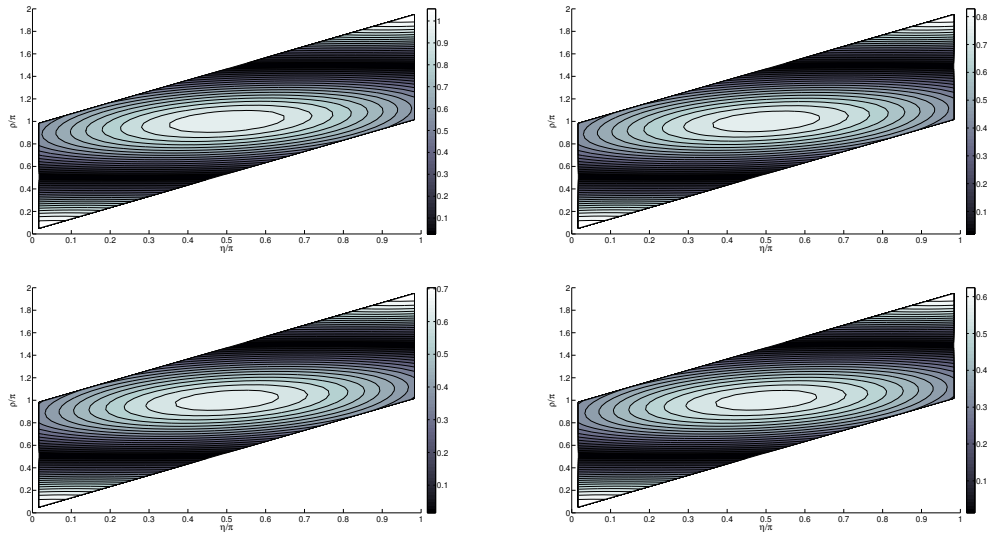

Figure 3.8: Convergence of $|\delta_1 - 1|$ as a function of η/π and ρ/π for SU(2) with adjoint fermions at $L = 6$ with $s = 2, 8/3, 10/3, 4$.

We have also plotted δ_1 with old and new boundary conditions for SU(2) and SU(3) with adjoint and SU(3) with sextet fermions for $s = 2, 3, 4$ as a function of a/L to see how the convergence is affected by the change of s. These are presented in figures 3.9, 3.10 and 3.11. All of these figures have the same qualitative behavior. While the convergence does improve slightly as s is increased, the change is still quite small and not enough to cure the higher order lattice effects present in the step scaling functions with the old boundary conditions.

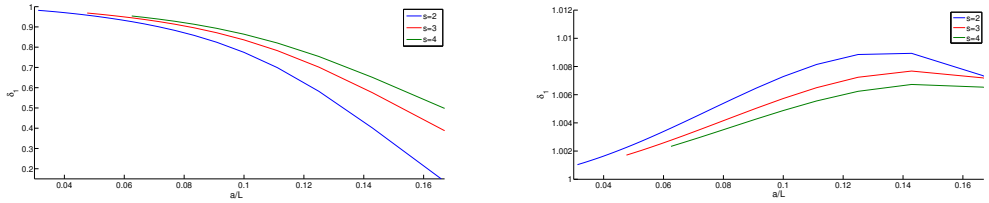

Figure 3.9: Fermionic parts of the Lattice step scaling function for SU(2) adjoint with old (left) and new (right) boundary conditions for $s = 2, 3, 4$.

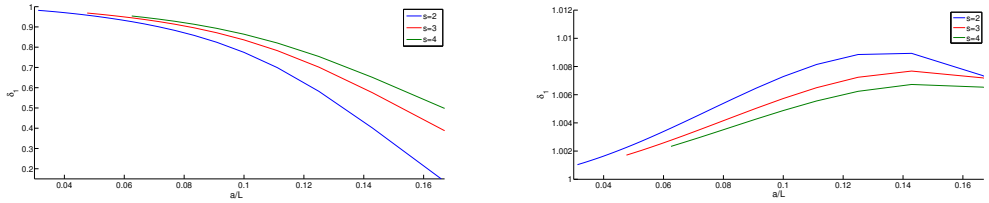

Figure 3.10: Fermionic parts of the Lattice step scaling function for SU(3) adjoint with old (left) and new (right) boundary conditions for $s = 2, 3, 4$.

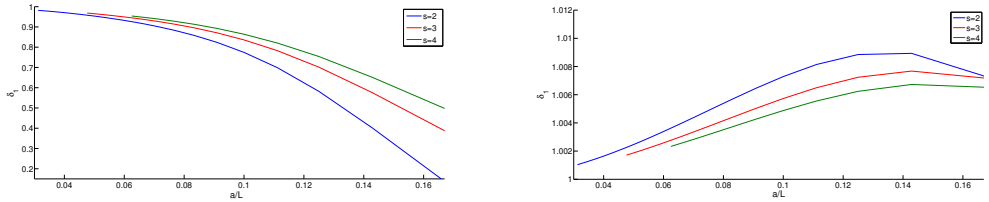

Figure 3.11: Fermionic parts of the Lattice step scaling function for SU(3) sextet with old (left) and new (right) boundary conditions for $s = 2, 3, 4$.

3.4 Fundamental representation

We wanted to check that the same phenomenon also occurs with the fundamental representation fermions. It turns out that this is true, as can be seen from figure 3.12. Thus the standard boundary conditions are selected so that the higher order lattice artifacts cancel.

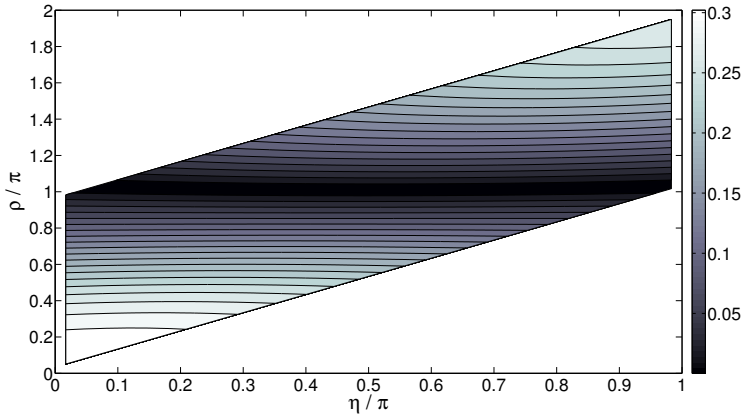

Figure 3.12: Convergence of $|\delta_1 - 1|$ as a function of η/π and ρ/π for SU(2) with fundamental fermions at $L = 10$. The conventional choice is $\rho = \pi$ and $\eta = \frac{\pi}{4}$.

3.5 Gauge sector

One has to keep in mind that changing the boundary conditions could in principle also affect the convergence of the gauge part of the step scaling function. This also happens to be true, but fortunately the effects are roughly one hundred times smaller. Thus one can freely choose the boundary conditions that are optimal for the fermionic part without compromising the convergence of the step scaling function.

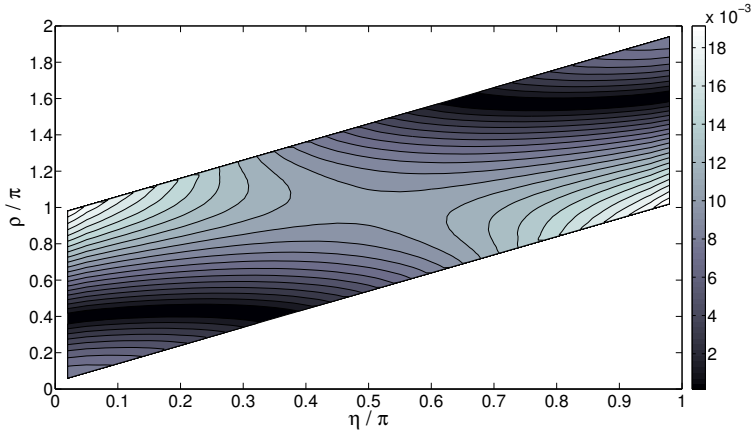

Figure 3.13: Convergence of $|\delta_0 - 1|$ as a function of η/π and ρ/π for SU(2) at $L = 10$.

In fact for the gauge part of SU(2) the convergence is even faster if one uses the new boundary conditions that are optimized for the adjoint fermions. This can be seen from figure 3.14 where δ_0 is plotted as a function of a/L with old and new boundary conditions.

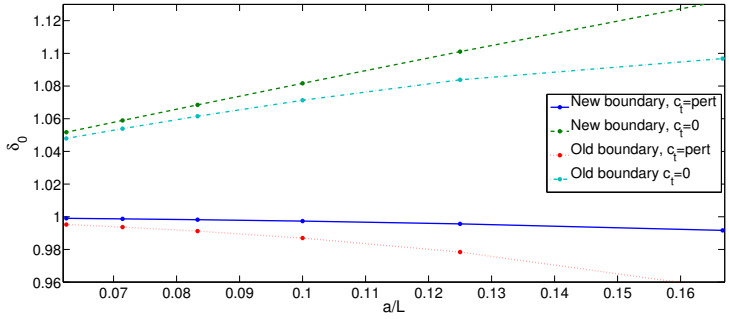

Figure 3.14: Gauge part of the Lattice step scaling function for SU(2) with old and new boundary conditions for adjoint fermions.

Chapter 4

Lattice simulations of SU(2) gauge theory with $N_{\mathrm{F}} = 4$, 6 and 10

In this chapter we will go through the simulation methods used in [III] and the main results for the SU(2) simulations with 4, 6 and 10 fermions.

4.1 Preliminaries

We are interested in the scaling properties of the coupling constant and the possible existence of a nontrivial IRFP as well as the anomalous dimension of the mass operator at the fixed point. We use the Schrödinger functional introduced in section 2.2 to carry out the necessary measurements.

Evolution of the coupling can easily be quantified with the step scaling function from equation (3.2). The step scaling function can be related to the beta function via

$$-2\ln(s) \;=\; \int_{u}^{\sigma(u,s)} \frac{dx}{\sqrt{x}\beta(\sqrt{x})}. \tag{4.1}$$

Near the fixed point β-function is small and (4.1) can be approximated with

$$\beta(g) \;\approx\; \frac{g}{2\ln(2)}\left(1 - \frac{\sigma(g^2,s)}{g^2}\right). \tag{4.2}$$

We also measured the mass anomalous dimension $\gamma = -d\ln m_q / d\ln\mu$ of the $N_{\mathrm{F}} = 6$ theory using the pseudoscalar density renormalization constant which is defined as

$$Z_P(L) = \frac{\sqrt{3} f_1}{f_P(L/2)}, \tag{4.3}$$

where

$$f_1 = -\frac{1}{12L^6}\int d^3u d^3v d^3y d^3z \langle \bar{\zeta}'(u)\gamma_5\lambda^a\zeta'(v)\bar{\zeta}(y)\gamma_5\lambda^a\zeta(z)\rangle, \tag{4.4}$$

$$f_P(x_0) = -\frac{1}{12L^6}\int d^3y d^3z \langle \bar{\psi}(x_0)\gamma_5\lambda^a\psi(x_0)\bar{\zeta}(y)\gamma_5\lambda^a\zeta(z)\rangle, \tag{4.5}$$

are correlation functions of the pseudoscalar density. Here sources ζ and ζ' are located at the $t = 0$ and $t = L$ boundaries, respectively. For these measurements the boundary matrices at $t = 0$ and $t = L$ were set to unity. The mass step scaling function is then defined as [67]:

$$\Sigma_P(u, s, L/a) = \left.\frac{Z_P(g_0, sL/a)}{Z_P(g_0, L/a)}\right|_{g^2(g_0,L/a)=u}, \tag{4.6}$$

$$\sigma_P(u, s) = \lim_{a/L\to 0} \Sigma_P(u, s, L/a), \tag{4.7}$$

and we chose again $s = 2$. We found the continuum step scaling function σ_P by measuring Σ_P at $L/a = 6$ and 10, and doing a quadratic extrapolation. It can be related to the anomalous dimension of the mass operator by [68]

$$\sigma_P(u, s) = \left(\frac{u}{\sigma(u, s)}\right)^{-d_0/(2b_0)} \exp\left[\int_{\sqrt{u}}^{\sqrt{\sigma(u,s)}} dx \left(\frac{\gamma(x)}{\beta(x)} - \frac{d_0}{b_0 x}\right)\right], \tag{4.8}$$

where $b_0 = \beta_0/(16\pi^2)$ in terms of the one-loop coefficient β_0 of the beta function and $d_0 = -8/(16\pi^2)$ is the corresponding one-loop coefficient for the anomalous dimension $\gamma = d_0 g^2$. This can be approximated at the fixed point with

$$\gamma^*(g^2) = \frac{\sigma_P(g^2, s)}{\log(s)}. \tag{4.9}$$

We set the improvement coefficient $c_{\rm sw}$ to its perturbative value [56] $c_{\rm sw} = 1 + 0.1551(1)g_0^2 + O(g_0^4)$. To make sure that the perturbative value of $c_{\rm sw}$ is close to the non-perturbative one, we measured $c_{\rm sw}$ using techniques from [I]. We also included the perturbative improvement at the Schrödinger functional boundaries, which was discussed in chapter 2

4.2 Measurements

The zero mass limit was determined by measuring the $\kappa_c = 1/(8 + 2m_{0,c})$ for all the used values of β via the PCAC relation using lattice size 16^4. The measured values of κ_c, given in table 4.1, were then used for all lattice sizes. In practice we achieved $|aM| < 0.01$.

$N_{\rm F}=4$		
β_L	κ_c	N_{traj}
1.8	0.14162	108755
1.9	0.139914	89064
2	0.138638	55031
2.2	0.136636	13294
2.4	0.135205	23359
3	0.132548	64035
4	0.130326	58879

$N_{\rm F}=6$		
β_L	κ_c	N_{traj}
1.39	0.144351377	215119
1.4	0.139914	221273
1.44	0.14350583	209124
1.5	0.142446	233273
1.8	0.1385229	25886
2	0.1367336	54710
2.4	0.1342875	33818
3	0.132115	41221
4	0.13014328	47419
5	0.1290368	41440
8	0.1274578	7116

$N_{\rm F}=10$		
β_L	κ_c	N_{traj}
1	0.14199	216356
1.3	0.13922	232495
1.5	0.13762	100476
1.7	0.13627	99792
2	0.13466	213290
3	0.13146	99918
4	0.12981	100328
6	0.1282	98042
8	0.12739	99255

Table 4.1: Parameter κ used in the simulations at each $\beta_L = 4/g_0^2$ and the number of measurements performed on the largest lattice.

β_L	$L/a=6$	$L/a=8$	$L/a=12$	$L/a=16$
4	1.2394(18)	1.263(3)	1.300(3)	1.32(1)
3	1.832(5)	1.882(5)	1.971(18)	2.02(2)
2.4	2.629(7)	2.767(15)	2.94(2)	3.17(4)
2.2	3.113(7)	3.29(2)	3.58(3)	3.88(9)
2	3.93(2)	4.24(3)	4.77(8)	5.18(11)
1.9	4.65(2)	4.95(5)	5.48(7)	6.9(3)
1.8	5.78(4)	6.43(7)	8.15(17)	9.0(5)

Table 4.2: The measured values of g^2 at each $\beta_L = 4/g_0^2$ and L/a with 4 flavors of fermions.

β_L	$L/a=6$	$L/a=8$	$L/a=10$	$L/a=12$	$L/a=16$
8	0.5207(8)	0.5222(9)		0.5274(13)	0.528(4)
5	0.8585(15)	0.868(3)		0.875(3)	0.889(4)
4	1.095(3)	1.109(2)	1.112(4)	1.122(8)	1.135(7)
3	1.535(8)	1.555(10)		1.587(10)	1.623(15)
2.4	2.030(8)	2.087(16)		2.19(3)	2.25(4)
2	2.655(15)	2.84(6)	2.76(3)	2.95(5)	3.1(2)
1.8	3.25(3)	3.33(4)	3.45(5)	3.47(4)	3.57(11)
1.5	5.40(6)	5.59(6)	5.57(11)	5.75(11)	6.12(13)
1.44	7.21(10)	7.11(15)	7.2(3)	7.3(3)	7.5(2)
1.4	9.74(13)	9.82(13)	10.2(3)	9.8(3)	10.4(4)
1.39	11.48(16)	13.4(3)		13.5(6)	13.5(8)

Table 4.3: The measured values of g^2 at each β_L and L/a with 6 flavors of fermions.

β_L	$L/a = 6$	$L/a = 8$	$L/a = 12$	$L/a = 16$
8	0.4700(2)	0.4706(4)	0.4705(5)	0.4707(10)
6	0.6148(3)	0.6159(5)	0.6180(9)	0.6181(19)
4	0.8897(9)	0.8897(13)	0.895(4)	0.895(3)
3	1.1528(16)	1.156(3)	1.150(2)	1.146(4)
2	1.651(4)	1.653(5)	1.637(6)	1.624(13)
1.7	1.924(4)	1.907(5)	1.905(11)	1.896(13)
1.5	2.183(3)	2.137(7)	2.116(11)	2.10(2)
1.3	2.542(8)	2.473(9)	2.382(11)	2.37(2)
1	4.03(2)	3.55(2)	3.23(3)	3.09(4)

Table 4.4: The measured values of g^2 at each β_L and L/a with 10 flavors of fermions.

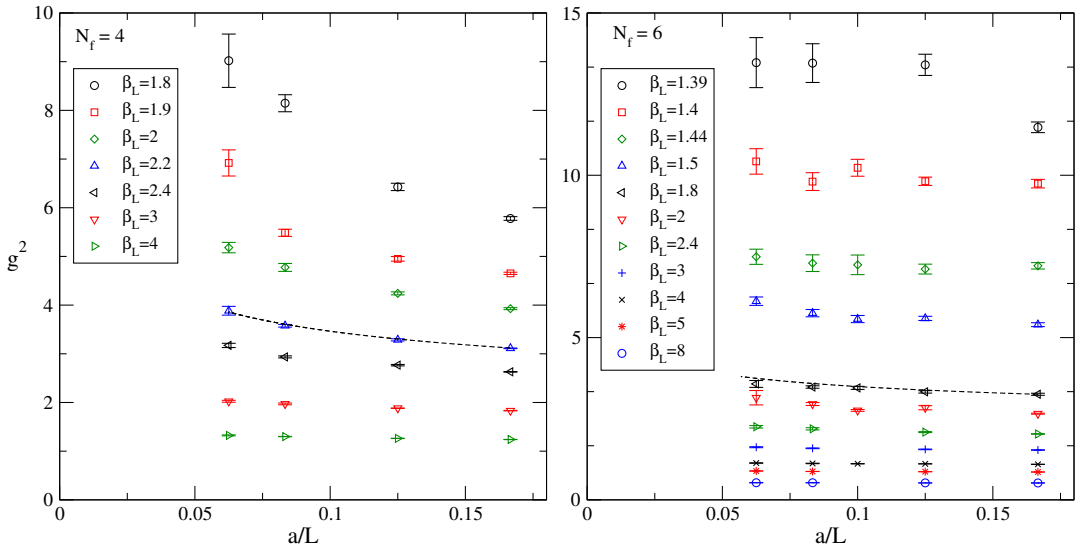

Figure 4.1: The measured values of $g^2(g_0^2, L/a)$ against a/L with 4 and 6 flavors of fermions. The black dashed line gives an example of the running in 2-loop perturbation theory at modest coupling, normalised so that it matches the measurement at $L/a = 6$.

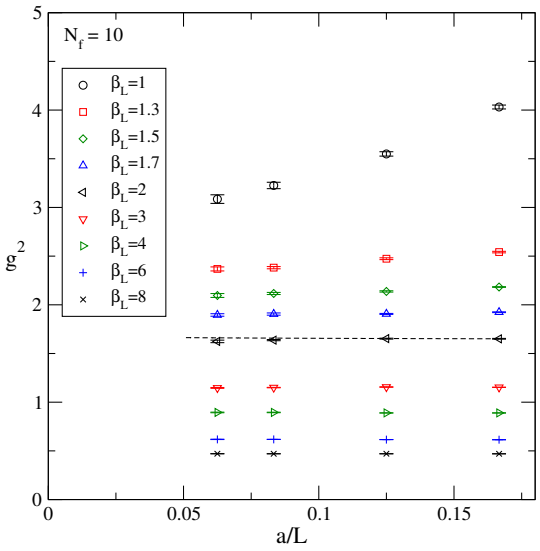

Figure 4.2: The measured values of $g^2(g_0^2, L/a)$ against a/L with 10 flavors of fermions. The black dashed line gives an example of the running in 2-loop perturbation theory.

The running coupling g was measured for a range in β_L using lattice sizes[1] 6^4, 8^4, 12^4 and 16^4. These results are shown in tables 4.2, 4.3 and 4.4. We have also plotted the measured values of g^2 as a function of a/L in figures 4.1 and 4.2. The measured values of g^2 were then used to find an interpolating function in g_0 of the form

$$\frac{1}{g^2(g_0^2, L/a)} = \frac{1}{g_0^2}\left[\frac{1+\sum_{i=1}^{n} a_i g_0^{2i}}{1+\sum_{i=1}^{m} b_i g_0^{2i}}\right]. \tag{4.10}$$

For 4 and 6 fermions the number of terms were chosen to be $n = m = 2$ and for 10 fermions $n = 1$ and $m = 2$.[2] The stability of the fits was checked by varying n or m. The interpolating function was used to find the step scaling function for $L/a = 6, 8$, and the continuum limit was extracted using

$$\Sigma(u, 2, L/a) = \sigma(u, 2) + c\,(L/a)^2\,. \tag{4.11}$$

Because of the improved action we expect the $\mathcal{O}(a)$ terms to be subleading. Unfortunately, with only two points in the extrapolation, it was not possible to verify the accuracy of the extrapolation quantitatively.

The anomalous dimension of the mass operator was determined for the $N_{\mathrm{F}} = 6$ theory similarly. The pseudoscalar density renormalization constant Z_P was measured for a range in β and L/a. The values are presented in table 4.5.

[1] For $N_{\mathrm{F}} = 6$ the coupling was also measured with 10^4 lattice. This data was used in the measurement of γ

[2] For $N_{\mathrm{F}} = 10$ choosing $n = 2$ produces a singularity within the fitting range, which is not acceptable.

β_L	$L/a=6$	$L/a=8$	$L/a=10$	$L/a=12$	$L/a=16$	$L/a=20$
2.4	0.9666(8)	0.9353(9)	0.9171(19)	0.9014(19)	0.8870(15)	0.865(4)
2	0.8953(10)	0.857(3)	0.838(2)	0.823(3)	0.793(4)	0.766(6)
1.5	0.702(4)	0.669(3)	0.646(4)	0.618(6)	0.586(5)	0.573(6)
1.44	0.636(3)	0.610(3)	0.588(4)	0.572(4)	0.548(4)	0.517(6)
1.4	0.543(5)	0.547(5)	0.539(5)	0.534(5)	0.508(6)	0.480(8)
1.39	0.508(5)	0.515(7)	0.520(6)	0.517(6)	0.488(8)	0.476(9)

Table 4.5: The measured values of Z_P at each β_L and L with 6 flavors of fermions.

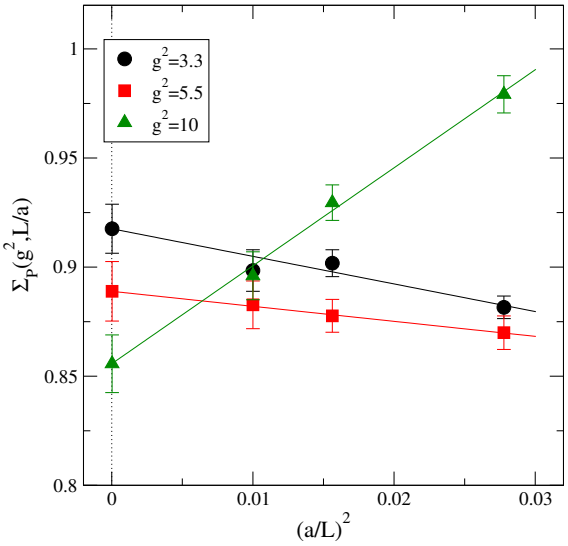

Figure 4.3: The mass step scaling function extrapolated to the continuum limit, using $N_f = 6$ data and shown for three chosen values of g^2.

The data was used to find an interpolating function of the form

$$Z_P(\beta, L/a) = \sum_{i=0}^{n} c_i \left(\frac{1}{\beta}\right)^i \tag{4.12}$$

with $c_0 = 1$, where we have truncated the series at $n = 4$. From the interpolated $Z_p(\beta_L, L/a)$ we obtained the mass step scaling function $\Sigma_P(u, s, L/a)$ at $L/a = 6, 8$ and 10 using (4.6), using $u = g^2$ from rational fit (4.10). The continuum extrapolation was then done by fitting to the extrapolating function

$$\Sigma_P(u, 2, L/a) = \sigma_P(u, 2) + c(u)\,(L/a)^{-2}\,. \tag{4.13}$$

The fit is shown in figure 4.3. Step scaling function was converted to the estimate of the anomalous dimension using (4.9), and the results are shown in figure 4.4.

The mass anomalous dimension we measured is somewhat smaller than the perturbative one at strong coupling. It remains small at all measured values of the coupling, and if there is a fixed point at $g^2 \gtrsim 12$, the anomalous dimension is $\gtrsim 0.25$.

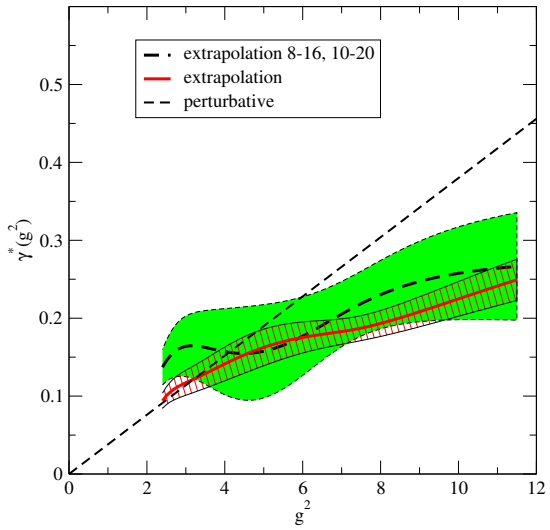

Figure 4.4: The estimate of the mass anomalous dimension, $\gamma^*(g^2)$, with $N_f = 6$. Shown are the continuum extrapolation using the mass step scaling $\Sigma(L/a, 2, g^2)$ with all three volumes $L/a = 6, 8, 10$ (hashed band) and only with $L/a = 8, 10$ (shaded band).

4.3 Results

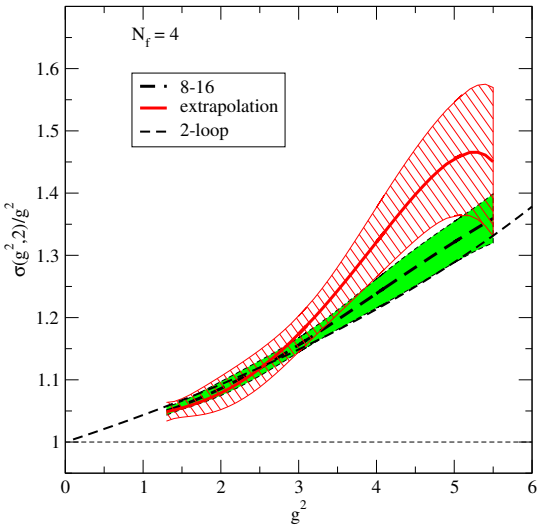

Figure 4.5: (colour online) The scaled step scaling function $\sigma(g^2, 2)/g^2$ with 4 fermions. The thick red line corresponds to the continuum extrapolation (4.11), and the hashed band to the statistical errors of the extrapolation. The thick dashed line with the shaded error band is the largest volume step scaling function without extrapolation. The thin dashed line is the 2-loop perturbative value of $\sigma(g^2, 2)/g^2$.

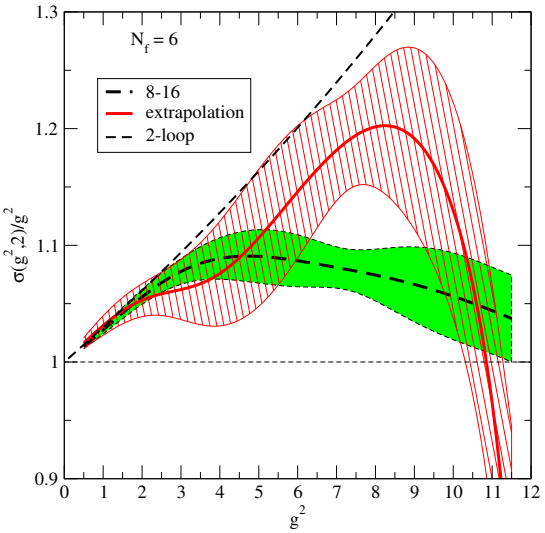

Figure 4.6: As in figure 4.5 but with 6 fermion flavors.

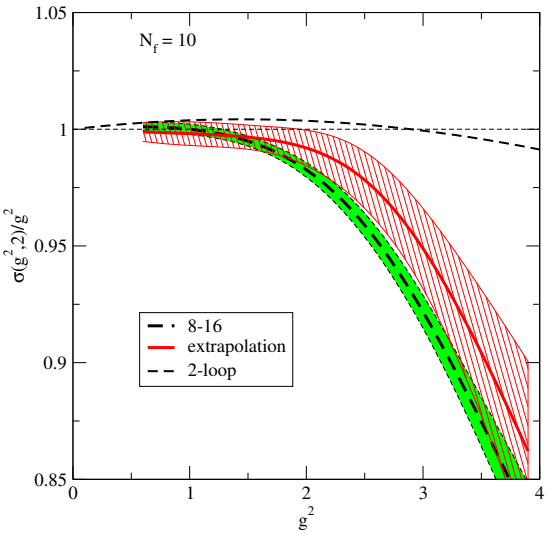

Figure 4.7: As in figure 4.5 but with 10 fermion flavors.

In figures 4.5, 4.6 and 4.7 we show the step scaling functions. In the $N_{\rm F} = 10$ theory the evolution of the coupling is extremely slow, and our results basically agree with this at $g^2 \lesssim 2.5$: the step scaling practically vanishes in this range. In this case we expect the two-loop perturbative step scaling function to be fairly accurate, and from figure 4.7 we see that the errors should be an order of magnitude smaller in order to resolve it. At stronger coupling the measured step scaling deviates significantly from zero to negative values. Combined with the analytically known weak coupling behavior, this indicates that the β-function must have a fixed point somewhere in this range. However, we believe that a large fraction of the observed deviation from the perturbative step scaling at

strong coupling arises from the results at our strongest lattice coupling $\beta_L = 4/g_0^2 = 1$. This point deviates clearly from the rest of the simulation points, possibly indicating stronger cutoff effects.

Our simulations verify that the SU(2) gauge theory with 6 flavors of fundamental representation fermions is indeed close to the lower edge of the conformal window. Unfortunately, the possible fixed point in this theory is at such a strong coupling that we were not able to fully resolve the behavior: the results are compatible either with a fixed point at $g^2 \gtrsim 12$ or with a "walking" behavior where the β-function almost vanishes. The value of the fixed point coupling is naturally scheme dependent; this value is for the Schrödinger functional scheme. Resolving this question requires simulations with an action that can be used at stronger lattice couplings.

Chapter 5

Summary and outlook

The masses of the weak gauge bosons and fermions are included to the SM via the Higgs mechanism. However, the mathematical formulation of a fundamental scalar field, such as the Higgs field, suffers from naturality- and fine tuning problems. These can be overcome if the the Higgs sector of SM is replaced with a new strongly interacting gauge sector. As a consequence, the Higgs boson is a composite object of two fermionic fields. This is the basic idea of TC.

For TC to agree with the experimental data, the theory has to be nearly conformal and the anomalous dimension of the mass operator has to be of the order one. This motivates the search for a gauge field theory with these properties. Because we are studying strongly interacting field theories, the only reliable tool is lattice simulations.

The Wilson action and the Schrödinger functional provide a well established method of measuring the scale dependence of the coupling constant on the lattice. This has previously been used for SU(2) and SU(3) gauge theories with fundamental representation fermions. As we have shown, the Wilson fermions and the Schrödinger functional boundary conditions will introduce $\mathcal{O}(a)$ errors to the lattice action. These must be removed with proper counter terms for which corresponding coefficients must be determined perturbatively or non-perturbatively in order to cancel the unwanted effects. In this thesis we have calculated the previously unknown necessary improvement coefficients for higher representation fermions in SU(2) and SU(3).

The higher representation fermions will also introduce large $\mathcal{O}(a^2)$ errors to the perturbative step scaling function, the lattice equivalent of the β-function. These effects are absent if one uses fundamental representation fermions. We have shown that these effects can be removed with a careful choice of the Schrödinger functional boundary conditions, and provided suitable boundary fields for different representations of SU(2) and SU(3). This method, however, tends to reduce the signal from the coupling measurement.

We applied these methods to SU(2) gauge theory with 4, 6 and 10 fundamental fermions. We found that $N_{\mathrm{F}} = 4$ theory is QCD like, as is expected from the perturbative calculations. $N_{\mathrm{F}} = 6$ theory shows possible evidence of

an IRFP, but we were unable to simulate with sufficiently large lattice couplings to verify this. With $N_{\mathrm{F}} = 10$, our data is compatible with an IRFP. We also measured the anomalous dimension of the mass operator for the $N_{\mathrm{F}} = 6$ theory and found it to be $\gamma^* \approx 0.25$ at the possible fixed point around $g^2 \approx 12$.

The research done for this thesis continues. There is still work to do with the improvement coefficients and boundary conditions for different gauge groups and representations, such as SU(4). It has also be shown in [59] that the problem with $\mathcal{O}(a^2)$ terms in step scaling function can also be overcome with redefinition of the gauge coupling. A mixture of optimally defined coupling and boundary conditions might even boost the signal for the coupling measurements, thus improving the quality of the results remarkably.

These methods should then be applied to different theories within the conformal window to find viable candidates for walking TC. Simulations at finite temperature could also give us more insight to the nature of these theories.

Bibliography

[I] T. Karavirta, A. Mykkanen, J. Rantaharju, K. Rummukainen and K. Tuominen, JHEP **1106**, 061 (2011) [arXiv:1101.0154 [hep-lat]].

[II] T. Karavirta, K. Rummukainen and K. Tuominen, Phys. Rev. D **85**, 054506 (2012) [arXiv:1201.1883 [hep-lat]].

[III] T. Karavirta, J. Rantaharju, K. Rummukainen and K. Tuominen, JHEP **1205**, 003 (2012) [arXiv:1111.4104 [hep-lat]].

[1] P. W. Higgs, Phys. Lett. **12**, 132 (1964).

[2] P. W. Higgs, Phys. Rev. Lett. **13**, 508 (1964).

[3] S. Weinberg, Phys. Rev. Lett. **19**, 1264 (1967).

[4] A. Salam, Conf. Proc. C **680519**, 367 (1968).

[5] S. L. Glashow, J. Iliopoulos and L. Maiani, Phys. Rev. D **2**, 1285 (1970).

[6] G. Aad *et al.* [ATLAS Collaboration], Phys. Lett. B **716**, 1 (2012) [arXiv:1207.7214 [hep-ex]].

[7] S. Chatrchyan *et al.* [CMS Collaboration], Phys. Lett. B **716**, 30 (2012) [arXiv:1207.7235 [hep-ex]].

[8] L. Susskind, Phys. Rev. D **20**, 2619 (1979).

[9] S. Weinberg, Phys. Rev. D **19**, 1277 (1979).

[10] C. T. Hill and E. H. Simmons, Phys. Rept. **381**, 235 (2003) [Erratum-ibid. **390**, 553 (2004)] [hep-ph/0203079].

[11] F. Sannino, Acta Phys. Polon. B **40**, 3533 (2009) [arXiv:0911.0931 [hep-ph]].

[12] S. Dimopoulos and L. Susskind, Nucl. Phys. B **155**, 237 (1979).

[13] E. Eichten and K. D. Lane, Phys. Lett. B **90**, 125 (1980).

[14] K. Yamawaki, hep-ph/9603293.

[15] A. G. Cohen and H. Georgi, Nucl. Phys. B **314**, 7 (1989).

[16] B. Holdom, Phys. Lett. B **150**, 301 (1985).

[17] K. Yamawaki, M. Bando and K. -i. Matumoto, Phys. Rev. Lett. **56**, 1335 (1986).

[18] T. Banks and A. Zaks, Nucl. Phys. B **196**, 189 (1982).

[19] T. W. Appelquist, D. Karabali and L. C. R. Wijewardhana, Phys. Rev. Lett. **57**, 957 (1986).

[20] F. Sannino and K. Tuominen, Phys. Rev. D **71**, 051901 (2005) [hep-ph/0405209].

[21] D. D. Dietrich and F. Sannino, Phys. Rev. D **75**, 085018 (2007) [hep-ph/0611341].

[22] S. Catterall and F. Sannino, Phys. Rev. D **76**, 034504 (2007) [arXiv:0705.1664 [hep-lat]].

[23] A. J. Hietanen, J. Rantaharju, K. Rummukainen and K. Tuominen, JHEP **0905**, 025 (2009) [arXiv:0812.1467 [hep-lat]]

[24] L. Del Debbio, A. Patella and C. Pica, Phys. Rev. D **81** (2010) 094503 [arXiv:0805.2058 [hep-lat]].

[25] S. Catterall, J. Giedt, F. Sannino and J. Schneible, JHEP **0811**, 009 (2008) [arXiv:0807.0792 [hep-lat]].

[26] A. J. Hietanen, K. Rummukainen and K. Tuominen, Phys. Rev. D **80**, 094504 (2009) [arXiv:0904.0864 [hep-lat]].

[27] F. Bursa, L. Del Debbio, L. Keegan, C. Pica and T. Pickup, Phys. Rev. D **81**, 014505 (2010) [arXiv:0910.4535 [hep-ph]];

[28] L. Del Debbio, B. Lucini, A. Patella, C. Pica and A. Rago, Phys. Rev. D **80**, 074507 (2009) [arXiv:0907.3896 [hep-lat]].

[29] L. Del Debbio, B. Lucini, A. Patella, C. Pica and A. Rago, Phys. Rev. D **82** (2010) 014510 [arXiv:1004.3206 [hep-lat]].

[30] L. Del Debbio, B. Lucini, A. Patella, C. Pica and A. Rago, Phys. Rev. D **82** (2010) 014509 [arXiv:1004.3197 [hep-lat]].

[31] F. Bursa, L. Del Debbio, D. Henty, E. Kerrane, B. Lucini, A. Patella, C. Pica, T. Pickup *et al.*, [arXiv:1104.4301 [hep-lat]].

[32] T. DeGrand, Y. Shamir, B. Svetitsky, [arXiv:1102.2843 [hep-lat]].

[33] E. Kerrane *et al.*, arXiv:1011.0607 [hep-lat].

[34] Y. Shamir, B. Svetitsky and T. DeGrand, Phys. Rev. D **78**, 031502 (2008) [arXiv:0803.1707 [hep-lat]];

[35] T. DeGrand, Y. Shamir and B. Svetitsky, Phys. Rev. D **79**, 034501 (2009) [arXiv:0812.1427 [hep-lat]];

[36] T. DeGrand, Y. Shamir and B. Svetitsky, Phys. Rev. D **82**, 054503 (2010) [arXiv:1006.0707 [hep-lat]].

[37] Z. Fodor, K. Holland, J. Kuti, D. Nogradi and C. Schroeder, JHEP **0911**, 103 (2009) [arXiv:0908.2466 [hep-lat]].

[38] J. B. Kogut and D. K. Sinclair, Phys. Rev. D **81**, 114507 (2010) [arXiv:1002.2988 [hep-lat]].

[39] P. H. Damgaard, U. M. Heller, A. Krasnitz and P. Olesen, Phys. Lett. B **400**, 169 (1997) [arXiv:hep-lat/9701008].

[40] T. Appelquist, G. T. Fleming and E. T. Neil, Phys. Rev. Lett. **100**, 171607 (2008) [arXiv:0712.0609 [hep-ph]].

[41] T. Appelquist, G. T. Fleming and E. T. Neil, Phys. Rev. D **79**, 076010 (2009) [arXiv:0901.3766 [hep-ph]].

[42] Z. Fodor, K. Holland, J. Kuti, D. Nogradi and C. Schroeder, Phys. Lett. B **681**, 353 (2009) [arXiv:0907.4562 [hep-lat]];

[43] A. Deuzeman, M. P. Lombardo and E. Pallante, Phys. Lett. B **670**, 41 (2008) [arXiv:0804.2905 [hep-lat]];

[44] A. Deuzeman, M. P. Lombardo and E. Pallante, Phys. Rev. D **82**, 074503 (2010) [arXiv:0904.4662 [hep-ph]];

[45] E. Itou *et al.*, arXiv:1011.0516 [hep-lat].

[46] X. Y. Jin and R. D. Mawhinney, PoS **LATTICE2010**, 055 (2010) [arXiv:1011.1511 [hep-lat]].

[47] M. Hayakawa, K. I. Ishikawa, Y. Osaki, S. Takeda, S. Uno and N. Yamada, arXiv:1011.2577 [hep-lat].

[48] A. Hasenfratz, Phys. Rev. D **82**, 014506 (2010) [arXiv:1004.1004 [hep-lat]].

[49] A. Hasenfratz, Phys. Rev. D **80**, 034505 (2009) [arXiv:0907.0919 [hep-lat]].

[50] F. Bursa, L. Del Debbio, L. Keegan, C. Pica and T. Pickup, arXiv:1010.0901 [hep-ph].

[51] H. Ohki *et al.*, arXiv:1011.0373 [hep-lat].

[52] G. Voronov *et al.* (Lattice strong dynamics collaboration): Talk at LATTICE 2011, Squaw Valley, July 12 2011.

[53] K. G. Wilson, Phys. Rev. D **10**, 2445 (1974).

[54] B. Sheikholeslami and R. Wohlert, Nucl. Phys. B **259**, 572 (1985).

[55] R. Wohlert, DESY87/069

[56] M. Luscher and P. Weisz, Nucl. Phys. B **479**, 429 (1996) [arXiv:hep-lat/9606016].

[57] M. Luscher, S. Sint, R. Sommer, P. Weisz and U. Wolff, Nucl. Phys. B **491**, 323 (1997) [hep-lat/9609035].

[58] S. Sint, Nucl. Phys. B **451**, 416 (1995) [hep-lat/9504005].

[59] S. Sint and P. Vilaseca, arXiv:1211.0411 [hep-lat].

[60] M. Luscher, R. Narayanan, P. Weisz and U. Wolff, Nucl. Phys. B **384**, 168 (1992) [arXiv:hep-lat/9207009].

[61] M. Luscher, S. Sint, R. Sommer and P. Weisz, Nucl. Phys. B **478**, 365 (1996) [arXiv:hep-lat/9605038].

[62] M. Luscher, R. Sommer, P. Weisz and U. Wolff, Nucl. Phys. B **413**, 481 (1994) [arXiv:hep-lat/9309005].

[63] S. Sint and R. Sommer, Nucl. Phys. B **465**, 71 (1996) [arXiv:hep-lat/9508012].

[64] M. Luscher and P. Weisz, Nucl. Phys. B **266**, 309 (1986).

[65]

[65] R. Sommer, Nucl. Phys. Proc. Suppl. **60A**, 279 (1998) [arXiv:hep-lat/9705026].

[66] S. Sint and P. Vilaseca, PoS LATTICE **2011**, 091 (2011) [arXiv:1111.2227 [hep-lat]].

[67] S. Capitani *et al.* [ALPHA Collaboration], Nucl. Phys. B **544**, 669 (1999) [hep-lat/9810063].

[68] M. Della Morte *et al.* [ALPHA Collaboration], Nucl. Phys. B **729**, 117 (2005) [hep-lat/0507035].

Paper I

Nonperturbative improvement of SU(2) lattice gauge theory with adjoint or fundamental flavors
T. Karavirta, A. Mykkanen, J. Rantaharju, K. Rummukainen and K. Tuominen, JHEP **1106**, 061 (2011) [arXiv:1101.0154 [hep-lat]].

Paper II

Perturbative Improvement of the Schrodinger Functional for Lattice Strong Dynamics
T. Karavirta, K. Rummukainen and K. Tuominen,
Phys. Rev. D **85**, 054506 (2012) [arXiv:1201.1883 [hep-lat]].

Paper III

Determining the conformal window: SU(2) gauge theory with N_f = 4, 6 and 10 fermion flavours
T. Karavirta, J. Rantaharju, K. Rummukainen and K. Tuominen, arXiv:1111.4104 [hep-lat].